Dual-reactive B cells are autoreactive and highly enriched in the plasmablast and memory B cell subsets of autoimmune mice

Emilie M. Fournier, Maria-Gabriela Velez, Katelyn Leahy, Cristina L. Swanson, Anatoly V. Rubtsov, Raul M. Torres, and Roberta Pelanda

Integrated Department of Immunology, National Jewish Health and University of Colorado, Denver School of Medicine, Denver, CO 80206

Rare dual-reactive B cells expressing two types of Ig light or heavy chains have been shown to participate in immune responses and differentiate into IgG$^+$ cells in healthy mice. These cells are generated more often in autoreactive mice, leading us to hypothesize they might be relevant in autoimmunity. Using mice bearing *Igk* allotypic markers and a wild-type Ig repertoire, we demonstrate that the generation of dual-κ B cells increases with age and disease progression in autoimmune-prone MRL and MRL/*lpr* mice. These dual-reactive cells express markers of activation and are more frequently autoreactive than single-reactive B cells. Moreover, dual-κ B cells represent up to half of plasmablasts and memory B cells in autoimmune mice, whereas they remain infrequent in healthy mice. Differentiation of dual-κ B cells into plasmablasts is driven by MRL genes, whereas the maintenance of IgG$^+$ cells is partly dependent on Fas inactivation. Furthermore, dual-κ B cells that differentiate into plasmablasts retain the capacity to secrete autoantibodies. Overall, our study indicates that dual-reactive B cells significantly contribute to the plasmablast and memory B cell populations of autoimmune-prone mice suggesting a role in autoimmunity.

CORRESPONDENCE
Roberta Pelanda:
pelandar@njhealth.org

Abbreviations used: FO, follicular; MZ, marginal zone; PC, plasma cell.

While developing in the BM, B cells undergo stochastic rearrangement of Ig heavy (IgH) and Ig light (IgL) chain V(D)J gene segments resulting in the random expression of Ig H and L (κ and λ) chains in the emerging B cell population (Schlissel, 2003; Nemazee, 2006). During V(D)J recombination, allelic and isotypic exclusion at the Ig loci are also established, leading to the expression of a unique H and L chain pair and, therefore, of BCRs with unique specificity in each B cell (Langman and Cohn, 2002; Nemazee, 2006; Vettermann and Schlissel, 2010). These mechanisms ensure that developing B cells expressing BCRs reactive with self-antigens (i.e., autoreactive B cells) undergo tolerance induction, whereas those expressing BCRs specific for a foreign antigen or a peripheral self-antigen proceed in differentiation and selection into the periphery (Burnet, 1959). Autoreactive B cells are silenced by central tolerance in the BM via receptor editing and, less frequently, clonal deletion (Halverson et al., 2004; Ait-Azzouzene et al., 2005), whereas peripheral B cell tolerance proceeds via anergy and clonal deletion (Goodnow et al., 2005; Pelanda and Torres, 2006, 2012; Shlomchik, 2008). Despite these tolerance mechanisms, small numbers of autoreactive B cells are detected in peripheral tissues of healthy mice and humans (Grandien et al., 1994; Wardemann et al., 2003) and their numbers are increased in autoimmunity (Andrews et al., 1978; Izui et al., 1984; Warren et al., 1984; Samuels et al., 2005; Yurasov et al., 2005, 2006; Liang et al., 2009).

A small population of dual-reactive B cells expressing two types of L chains (or more rarely H chains) has been observed both in mice and humans (Nossal and Makela, 1962; Pauza et al., 1993; Giachino et al., 1995; Gerdes and Wabl, 2004; Rezanka et al., 2005; Casellas et al., 2007; Velez et al., 2007; Kalinina et al., 2011). These allelically and isotypically (overall haplotype)

M.-G. Velez's present address is Stanford University School of Medicine, Stanford, CA 94305.

The Rockefeller University Press $30.00
J. Exp. Med. 2012 Vol. 209 No. 10 1797-1812
www.jem.org/cgi/doi/10.1084/jem.20120332

The Journal of Experimental Medicine

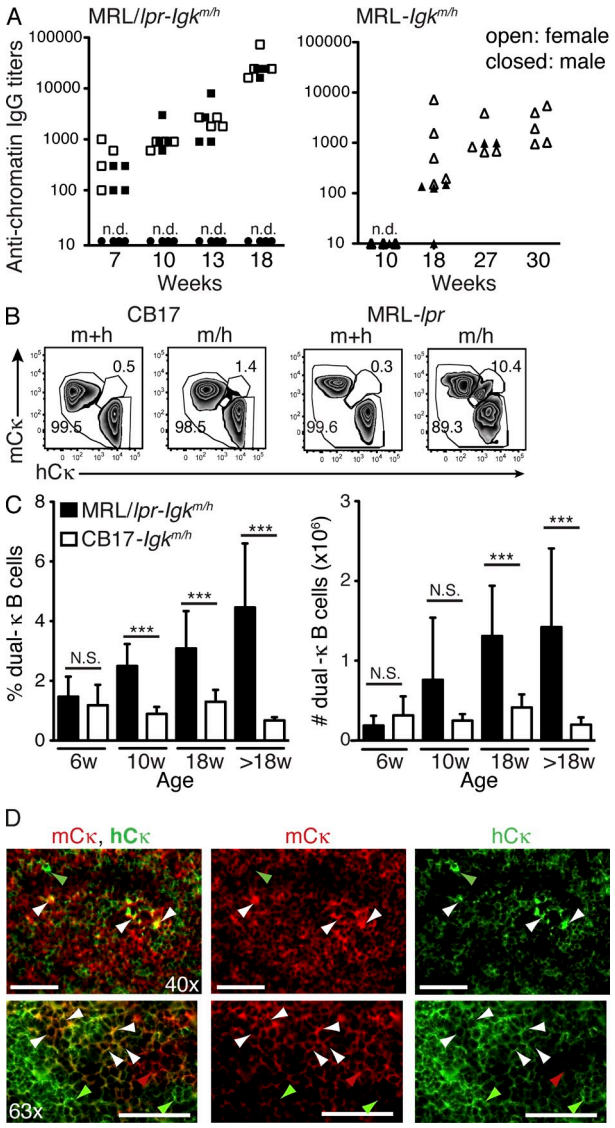

Figure 1. Frequency of dual-κ B cells increases with age in MRL/*lpr* mice. (A) Serum IgG titers of anti-chromatin antibodies in MRL/*lpr*-*lgk*$^{m/h}$ (squares, left), CB17-*lgk*$^{m/h}$ (circles, left), and MRL-*lgk*$^{m/h}$ (triangles, right). Mice were bled at the age indicated on the x-axis and sera tested for the presence of IgG anti-chromatin antibodies by ELISA. The serum antibody titer is defined as the dilution corresponding to an OD_{405} of 1. Each symbol represents an individual mouse, and females and males of MRL/*lpr*-*lgk*$^{m/h}$ and MRL-*lgk*$^{m/h}$ mice are identified by open and closed symbols, respectively. Sera were collected and frozen on different days and then analyzed together on the same day by ELISA to reduce intra-experimental variability. Data represent a total of $n = 6$ mice per group, analyzed in at least two independent experiments. n.d., not detected. (B) Spleen cells from 20-wk-old MRL/*lpr*-*lgk*$^{m/h}$ and CB17-*lgk*$^{m/h}$ mice (m/h) were analyzed by flow cytometry to detect and quantify dual-κ B cells. In parallel, mixtures of wild-type *lgk*$^{m/m}$ and homozygous *lgk*$^{h/h}$ mice (m+h) were analyzed to control for the presence of false dual-κ cell events. Zebra plots represent live single B220$^+$Igκ$^+$ gated B cells. Numbers are percentages of cells within each gate. This analysis is representative of at least three independent experiments. (C) Bar graphs represent mean frequencies ± SD (left) within the total B cell population and mean absolute numbers ± SD (right) of dual-κ B cells in the spleen of MRL/*lpr*-*lgk*$^{m/h}$ (black bars) and CB17-*lgk*$^{m/h}$ (white bars) mice at 6, 10, 18, and >18 wk of age. Data are from at least three independent experiments with a total combined of $n = 5$–10 mice per each age group. ***, $P < 0.0001$. N.S., not significant. (D) Representative histological analyses of Igκ$^+$ B cells in a MRL/*lpr*-*lgk*$^{m/h}$ mouse. LN sections were stained for mCκ (red) and hCκ (green). Middle and right panels show staining for only hCκ and mCκ, respectively. White arrowheads indicate representative dual-κ B cells, whereas green and red arrowheads point to representative single-κ B cells in the sections. Bars, 50 µm. Histological analyses were performed over at least three independent experiments on sections from three individual MRL/*lpr*-*lgk*$^{m/h}$ mice.

included B cells are <5% of all peripheral B cells in normal mice (Barreto and Cumano, 2000; Rezanka et al., 2005; Casellas et al., 2007; Velez et al., 2007), but they are more frequent in Ig knockin mice in which newly generated B cells are autoreactive and actively undergo receptor editing (Li et al., 2002a,b; Liu et al., 2005; Huang et al., 2006; Casellas et al., 2007). B cells that coexpress autoreactive and nonautoreactive antibodies can escape at least some of the mechanisms of central and peripheral B cell tolerance and be selected into the mature peripheral B cell population (Kenny et al., 2000; Li et al., 2002a,b; Gerdes and Wabl, 2004; Liu et al., 2005; Huang et al., 2006), sometimes with a preference for the marginal zone (MZ) B cell subset (Li et al., 2002b).

Furthermore, dual-reactive B cells observed within a normal polyclonal Ig repertoire exhibit characteristics of cells that develop through the receptor editing process, including delayed kinetics of differentiation and more frequent binding to self-antigens (Casellas et al., 2007). Hence, dual-reactive B cells might play a role in autoantibody generation and autoimmunity. However, the contribution of these B cells to autoimmunity has not yet been established. Our hypothesis is that haplotype-included autoreactive B cells are positively selected within the context of genetic backgrounds that manifest defects in immunological tolerance and contribute to the development of autoimmunity.

Until recently, the analysis of dual-reactive B cells was impaired by the inability to detect dual-κ cells, which are the most frequent among haplotype-included B cells (Casellas et al., 2007; Velez et al., 2007). To overcome this issue, we took advantage of *Igk*^{h} mice that bear a gene-targeted human *Ig Ck* allele in the context of a wild-type Ig repertoire (Casellas et al., 2001) and crossed these to MRL-*Fas*$^{lpr/lpr}$ (MRL/*lpr*) and MRL mice that develop an autoimmune pathology with characteristics similar to human lupus (Izui et al., 1984; Rordorf-Adam et al., 1985; Theofilopoulos and Dixon, 1985; Cohen and Eisenberg, 1991; Watanabe-Fukunaga et al., 1992). MRL/*lpr* mice, moreover, display defects in receptor editing (Li et al., 2002a; Lamoureux et al., 2007; Panigrahi et al., 2008) and reduced tolerance induction (Li et al., 2002a), which could potentially contribute to higher frequency of haplotype-included autoreactive B cells.

We found that the frequency of dual-κ cells increased with age and progression of disease in autoimmune-prone mice and independent of the expression of Fas. Dual-κ B cells exhibited higher prevalence of autoreactivity than single-κ B cells and were frequently selected into the antigen-activated cell subsets in MRL/*lpr* and MRL mice where up to half of

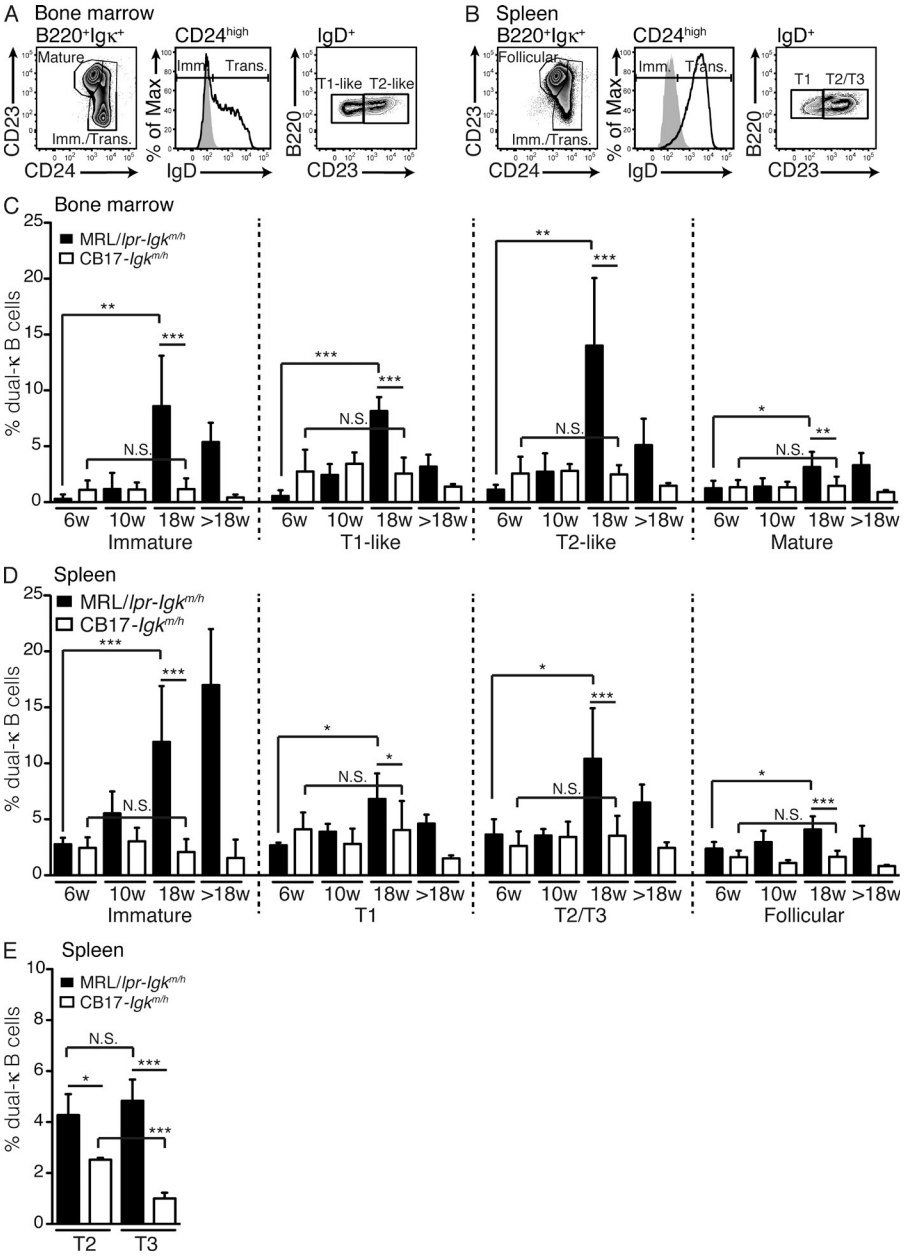

Figure 2. Generation of dual-κ B cells is increased in MRL/*lpr* mice. (A and B) Gating strategy to identify B cell subsets in BM (A) and spleen (B) is shown for a CB17-*Igk*$^{m/h}$ mouse. Cell gating in each plot is indicated on top. The following markers were used to discriminate B cells subsets: immature (imm.), CD24^{high}CD23^{-}IgD^{-}; transitional (trans.) T1-like (BM) and transitional T1 (spleen), CD24^{high}IgD^{+}CD23^{-}; transitional T2-like (BM) and transitional T2+T3 (spleen), CD24^{high}IgD^{+}CD23^{+}; mature (BM) and FO (spleen), CD24^{low}CD23^{+}IgD^{+}. This analysis is representative of at least three independent experiments. (C and D) Bar graphs represent mean frequencies ± SD of dual-κ B cells in indicated B cell subsets gated as shown in Fig. 2 (A and B) in BM (C) and spleen (D) of MRL/*lpr-Igk*$^{m/h}$ (black bars) and CB17-*Igk*$^{m/h}$ (white bars) mice at 6, 10, 18, and >18 wk of age. Data are from at least three independent experiments, with a total combined of n = 5–10 mice per age group. ***, P < 0.001; **, P < 0.01; *, P < 0.05. N.S., not significant. (E) Bar graphs represent mean frequencies ± SD of dual-κ B cells in the T2 (CD24^{high}CD23^{+}IgM^{high}) and T3 (CD24^{high}CD23^{+}IgM^{low}) transitional cell subsets in the spleen of MRL/*lpr-Igk*$^{m/h}$ (black bars) and CB17-*Igk*$^{m/h}$ (white bars) mice at 14–15 wk of age. Data are from two independent experiments, with a total combined of n = 4 mice per group. ***, P < 0.001; *, P < 0.05. N.S., not significant.

the plasmablasts and memory B cells were dual-κ B cells. Moreover, disruption of Fas expression appeared to mediate increased survival of dual-reactive memory B cells. Overall, these data indicate that dual-reactive B cells significantly contribute to the plasmablast and memory B cell populations of autoimmune-prone mice suggesting a role in the development of autoimmunity.

RESULTS

Dual-κ B cells accumulate with age and autoantibodies in MRL/*lpr-Igk*$^{m/h}$ mice

To study the fate of dual-reactive B cells in autoimmune-prone mice with a polyclonal antibody repertoire and assess the contribution of these cells to the development of disease, we backcrossed nonautoimmune CB17-*Igk*$^{m/h}$ mice (Casellas et al., 2001;Velez et al., 2007) to autoimmune-prone MRL/*lpr* mice to generate MRL/*lpr-Igk*$^{m/h}$ mice. Because of the presence of the *Igk*^{h} allele, B cells of MRL/*lpr-Igk*$^{m/h}$ mice that coexpress two κ chains can be identified by the simultaneous expression of mouse and human Cκ regions. Upon observing MRL/*lpr-Igk*$^{m/h}$ mice of different age and determining titers of IgG anti-chromatin autoantibodies (Fig. 1 A, left), we established four age groups of study: 6, 10, 18, and >18 wk. 6-wk-old mice had low titers of anti-chromatin autoantibodies with no other manifestations of disease, 10-wk-old mice had increased autoantibodies and also palpable enlarged axillary LNs, 18-wk-old mice developed dermatitis and visible engrossed inguinal and axillary LNs, and older mice displayed the highest autoantibody titers, skin necrosis, severe lymphadenopathy, and weight loss (Fig. 1 A and not depicted). The study groups incorporated mice of both sexes as no significant gender differences were observed (Fig. 1 A).

To determine whether a positive correlation exists between dual-reactive B cells and autoimmunity, we measured

the frequency of dual-κ and dual-κ/λ (dual-L chain) B cells in the spleen of autoimmune-prone (MRL/*lpr-Igk*$^{m/h}$) and healthy control (CB17-*Igk*$^{m/h}$) mice stratified by age. In our analyses, the percentage of dual-κ/λ cells in MRL/*lpr-Igk*$^{m/h}$ mice was too low to be measured reliably (unpublished data). In contrast, a clear dual-κ (mCκ^{+}hCκ^{+}) B cell population was visible in CB17-*Igk*$^{m/h}$ and MRL/*lpr-Igk*$^{m/h}$ mice and not in control cell mixtures (Fig. 1 B; Velez et al., 2007). We found that both frequency and absolute numbers of dual-κ spleen B cells were significantly higher in MRL/*lpr-Igk*$^{m/h}$ mice compared with CB17-*Igk*$^{m/h}$ mice starting at 10 wk of age and increasing with age and autoantibody titers (Fig. 1, A and C). Although an increase in the absolute numbers of dual-κ B cells in MRL/*lpr* mice is not particularly surprising given that the *Fas*^{lpr} mutation drives lymphoid expansion as a result of defects in apoptosis (Watanabe-Fukunaga et al., 1992), increased frequency of B cells that express two κ chains indicates a preferential expansion of the dual-κ B cell population relative to the single-κ population in autoimmune mice. The presence of dual-κ B cells in autoimmune mice was also supported by microscopic analyses of lymphoid tissue sections. Fluorescent microscopy of MRL/*lpr-Igk*$^{m/h}$ tissue sections detected cells coexpressing mouse and human κ constant regions within follicles (Fig. 1 D). Dual-κ B cells were not observed in sections from homozygous *Igk*$^{h/h}$ or *Igk*$^{m/m}$ mice and were much rarer in sections from CB17-*Igk*$^{m/h}$ mice (unpublished data). These results indicate that the frequency of dual-κ B cells increases in autoimmune-prone mice with disease progression.

Generation and positive selection of dual-κ B cells are augmented in autoimmune-prone MRL/*lpr* mice with age

To determine whether the increased frequency of dual-κ B cells in autoimmune mice was caused by a greater generation at the immature cell stage, or by expansion and/or maintenance at later cell developmental stages, we analyzed the frequency of dual-κ B cells in immature, transitional, and mature B cell populations in BM and spleen of MRL/*lpr-Igk*$^{m/h}$ and CB17-*Igk*$^{m/h}$ mice gated as shown in Fig. 2 (A and B). MRL/*lpr-Igk*$^{m/h}$ mice 18 wk of age and older exhibited a sharp increase in dual-κ B cells at every stage of B cell development examined compared with CB17 mice (Fig. 2, C and D). The frequency of dual-κ cells in older MRL/*lpr-Igk*$^{m/h}$ mice significantly decreased between the late transitional (T2-like and T2/T3) and the mature B cell stages both in BM and spleen (Fig. 2, C and D), suggesting the presence of active checkpoints of negative selection. However, the percentage of dual-κ B cells in the mature B cell population of MRL/*lpr-Igk*$^{m/h}$ mice was still significantly higher than that in CB17-*Igk*$^{m/h}$ mice, suggesting a selection advantage of these cells mediated by the autoimmune genetic background.

Transitional T3 B cells are considered anergic B cells that are arrested in development (Merrell et al., 2006). To clarify whether dual-κ B cells accumulate in this fraction, we performed additional flow cytometric analyses to resolve the T2 and T3 subsets. As shown in Fig. 2 E, dual-κ B cells were equally distributed in T2 and T3 fractions in MRL/*lpr-Igk*$^{m/h}$ mice, suggesting that half of these late transitional B cells might be anergic and unable to enter the mature B cell pool.

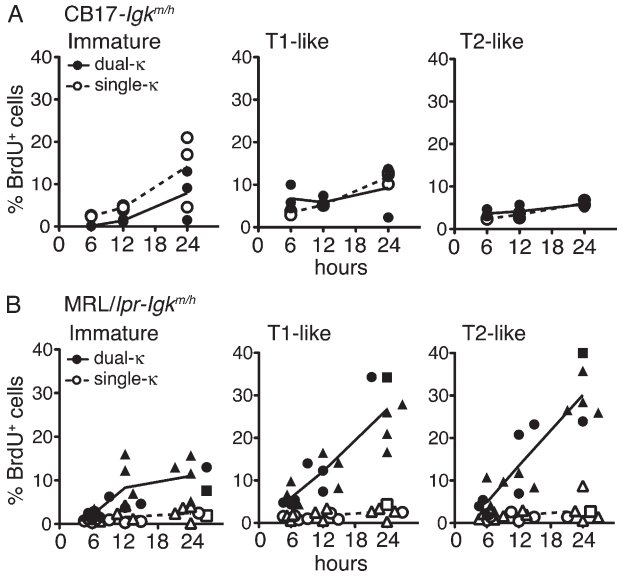

Figure 3. Dual-κ B cells display faster kinetics of differentiation in autoimmune-prone mice. (A and B) CB17-*Igk*$^{m/h}$ mice (20 wk of age) and MRL/*lpr-Igk*$^{m/h}$ mice (14–18 wk of age) were injected with BrdU at 0 and 12 h and analyzed 6, 12, or 24 h after the first injection to determine kinetics of BrdU labeling of immature and transitional BM B cells gated as in Fig. 2 A. Graphs represent the percentage of BrdU^{+} cells in dual-κ (closed symbols, solid line) and single-κ (open symbols, dashed line) cells in the indicated B cell subsets of individual CB17-*Igk*$^{m/h}$ and MRL/*lpr-Igk*$^{m/h}$ mice. Data for the MRL/*lpr-Igk*$^{m/h}$ mice were also stratified by the age of the animals: 14 wk (triangles), 15 wk (squares), and 18 wk (circles). Each symbol represents an individual mouse and lines are mean values. Data are from two independent experiments, with a total combined of $n = 3$–6 mice per strain and for each time point.

Overall, these data indicate that MRL/*lpr* mice produce larger amounts of immature dual-κ B cells, which likely contributes to an increased frequency of dual-κ mature B cells in autoimmune mice. However, most of the newly generated dual-κ B cells appear to be negatively selected during the differentiation into transitional, mature follicular (FO), and recirculating B cell stages.

Dual-κ B cells display faster kinetics of differentiation during development in MRL/*lpr* mice

We next examined the rate at which newly generated dual-κ B cells in MRL/*lpr* mice transit through the central selection checkpoints. For this analysis, we treated 14–18-wk-old CB17-*Igk*$^{m/h}$ and MRL/*lpr-Igk*$^{m/h}$ mice with BrdU and measured the kinetics of BrdU incorporation over 24 h in developing single and dual-κ B cells in the BM using an established method (Casellas et al., 2001, 2007; Hippen et al., 2005). As previously shown, the emergence of dual-κ cells in the immature B cell population of healthy CB17-*Igk*$^{m/h}$ mice was delayed relative to that of single-κ B cells (Fig. 3 A). In contrast, dual-κ B cells of lupus-prone MRL/*lpr-Igk*$^{m/h}$ mice

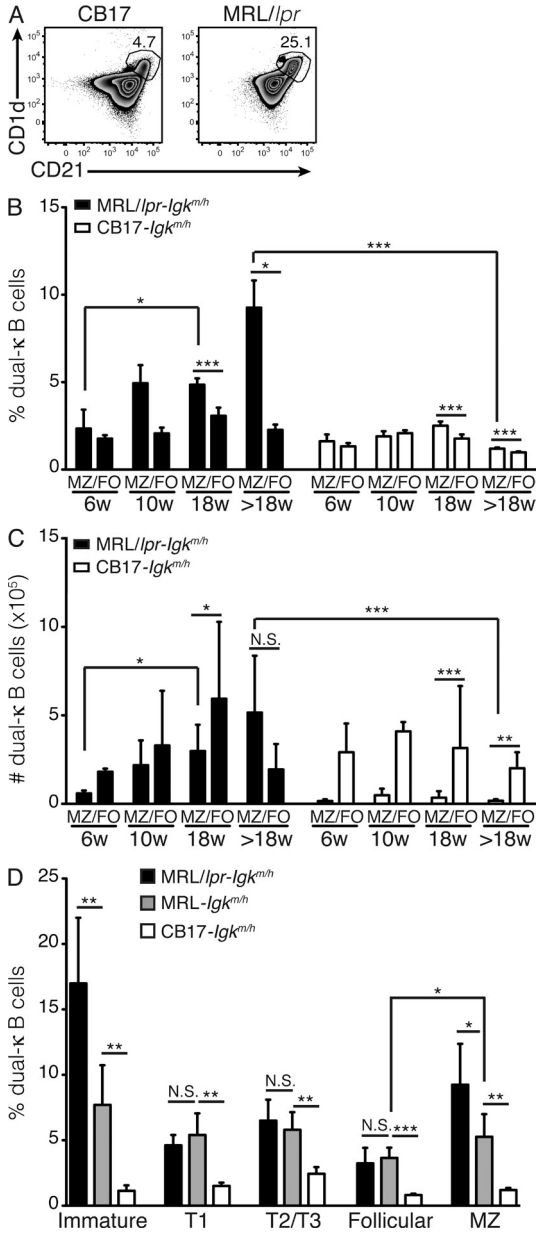

Figure 4. Dual-κ B cells are enriched in the MZ B cell subset and their increased production is mediated by the MRL genetic background. (A) Representative flow cytometric analysis of CD21^{+}CD1d^{high} MZ B cells in MRL/*lpr*-*Igk*$^{m/h}$ and CB17-*Igk*$^{m/h}$ mice. Numbers indicate frequencies of MZ B cells in live single B220^{+}Igκ^{+} gated cells. This analysis is representative of at least three independent experiments. (B and C) Bar graphs represent mean frequency ± SD (B) and mean absolute numbers ± SD (C) of dual-κ B cells in MZ and FO B cell subsets gated as in Fig. 2 B and Fig. 4 A in the spleen of MRL/*lpr*-*Igk*$^{m/h}$ (black bars) and CB17-*Igk*$^{m/h}$ (white bars) mice at 6, 10, 18, and >18 wk of age. Data are from at least three independent experiments, with a total combined of n = 4–10 mice per each age group. (D) Bar graph shows the mean frequency ± SD of dual-κ B cells in immature, transitional T1, transitional T2+T3, FO, and MZ B cells gated as in Fig. 2 (A and B) and Fig. 4 A in the spleen of MRL/*lpr*-*Igk*$^{m/h}$ (black bars), MRL-*Igk*$^{m/h}$ (gray bars), and CB17-*Igk*$^{m/h}$ (white bars) mice at 20–30 wk of age. Data are from at least three independent experiments with a total combined of n = 6–10 mice per group. ***, P < 0.001; **, P < 0.01; *, P < 0.05. N.S., not significant.

emerged in the immature B cell population before single-κ cells (Fig. 3 B), indicating an accelerated differentiation pathway from the preceding pre–B cell developmental stage. Moreover, this observation was independent of the age of the mice (Fig. 3 B). Higher kinetics of BrdU incorporation in dual-κ cells of autoimmune mice were also observed at the transitional B cell stages (Fig. 3 B). Surprisingly, the frequency of BrdU^{+} dual-κ B cells in the T1-like and T2-like B cell populations exceeded that in the immature B cell population, suggesting the presence of cell proliferation at the transitional cell stage. Overall, these data indicate that in contrast to healthy mice, dual-κ B cells in autoimmune-prone mice display faster kinetics of differentiation and/or increased cell proliferation relative to single-κ B cells.

Dual-κ B cells largely accumulate in the MZ B cell population in MRL/*lpr* mice

Dual-κ and κ/λ B cells have been shown to accumulate in the MZ B cell population of healthy mice (Li et al., 2002b; Casellas et al., 2007) although κ/λ anti-DNA B cells were found to be reduced in that of autoimmune MRL/*lpr* mice (Li et al., 2002a). We found that in a wild-type Ig repertoire, the frequency of MZ dual-κ B cells (gated as in Fig. 4 A) was significantly higher than that of FO B cells in both MRL/*lpr*-*Igk*$^{m/h}$ and CB17-*Igk*$^{m/h}$ mice older than 10 wk (Fig. 4 B). Moreover, consistent with differences observed in other B cell subsets, the frequency of dual-κ MZ B cells increased with age in MRL/*lpr*-*Igk*$^{m/h}$ mice and was significantly higher than that of CB17-*Igk*$^{m/h}$ mice (Fig. 4 B). In autoimmune mice older than 18 wk, dual-κ B cells were threefold more frequent in the MZ than in the FO B cell subset (Fig. 4 B) resulting in similar absolute cell numbers (Fig. 4 C). These data indicate that dual-κ B cells preferentially differentiate into MZ B cells in MRL/*lpr* autoimmune mice.

The MRL genetic background drives increased generation and selection of dual-κ B cells

The phenotype of MRL/*lpr* mice results from the contribution of both the MRL genetic background and the homozygous *Fas*^{lpr} mutation (Izui et al., 1984; Warren et al., 1984; Rordorf-Adam et al., 1985; Watanabe-Fukunaga et al., 1992; Ratkay et al., 1994; Nose et al., 1996; Kamogawa et al., 2002). To determine which of these genetic components is responsible for the increased generation of dual-κ B cells, we generated MRL-*Fas*$^{lpr/+}$-*Igk*$^{m/h}$ mice (referred to as MRL-*Igk*$^{m/h}$) that bear a wild-type *Fas* allele. These mice develop IgG anti-chromatin antibodies but, as expected, the kinetics of autoantibody appearance were delayed when compared with that of homozygous *Fas*$^{lpr/lpr}$ animals (Fig. 1 A). Similar to Fas-deficient mice, the frequency of dual-κ B cells in Fas-sufficient MRL-*Igk*$^{m/h}$ mice was significantly higher than that of CB17-*Igk*$^{m/h}$ mice in each of the B cell subsets examined and was only slightly lower in the immature and MZ B cell subsets relative to Fas-deficient MRL/*lpr* mice (Fig. 4 D). These data indicate that the MRL genetic background by itself drives increased generation of immature and mature dual-κ B cells.

Table 1. Generation of LPS-induced B cell hybridomas from MRL/*lpr-lgk*$^{m/h}$ and CB17-*lgk*$^{m/h}$ mice

Hybridomas	CB17-*lgk*$^{m/h}$	MRL/*lpr-lgk*$^{m/h}$
	n[a]	*n*[b]
Dual-κ	73	36
Dual-κ/λ	4	26
Total tested	2,288	873

[a]Hybridomas were obtained from six independent fusions of LPS-treated spleen cells from male and female CB17-*lgk*$^{m/h}$ mice of 6–10 wk of age.
[b]Hybridomas were from one fusion of LPS-treated spleen and LN cells from one 20-wk-old MRL/*lpr-lgk*$^{m/h}$ male.

Expression of autoantibodies is more frequent in dual-κ than in single-κ B cell hybridomas

To determine whether dual–L chain B cells express autoantibodies at higher frequency than single–L chain B cells, we generated a panel of LPS-induced B cell hybridomas from the spleen of MRL/*lpr-Igk*$^{m/h}$ and CB17-*Igk*$^{m/h}$ mice and considered it to represent the naive B cell population. Among these hybridomas we found several that coexpressed two L chains (Table 1). Approximately 20–50 single- and dual-κ hybridomas from each mouse strain were randomly selected to further analyze their self-reactivity toward HEp-2 antigens, chromatin, and Smith antigen. Clones were considered autoreactive when their reactivity toward self-antigen was three times above the SD of the negative control signal (Fig. 5 A). We found that dual-κ hybridomas were autoreactive more frequently (two- to threefold) than single-κ hybridomas for both MRL/*lpr-Igk*$^{m/h}$ and CB17-*Igk*$^{m/h}$ strains (Table 2) and in accordance with a previous analysis in healthy mice (Casellas et al., 2007). Not surprisingly, the overall frequency of autoreactive hybridomas from MRL/*lpr-Igk*$^{m/h}$ mice was greater than that of hybridomas from CB17-*Igk*$^{m/h}$ mice (Table 2).

To establish whether dual–L chain autoreactive B cell clones are also represented in the in vivo activated B cell population of MRL/*lpr* mice, we generated 816 spontaneous B cell hybridomas from nonmanipulated

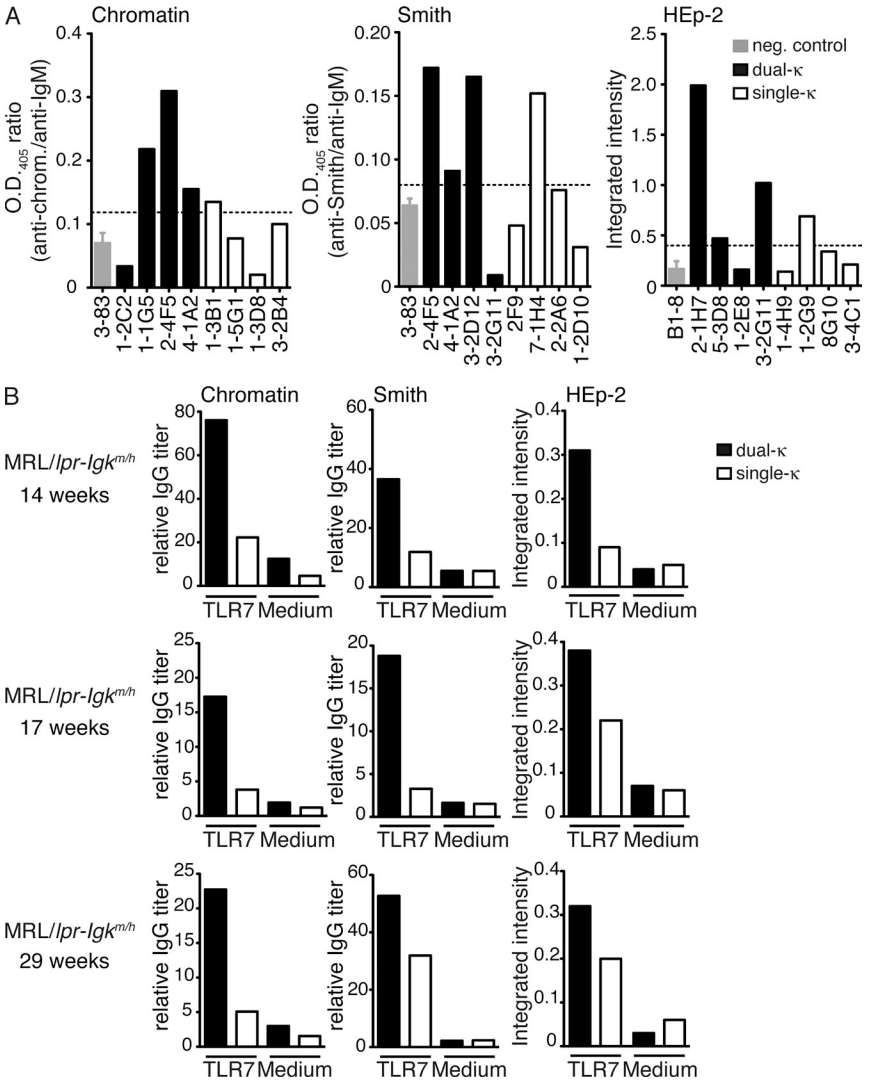

Figure 5. Dual-κ B cells secrete autoantibodies. (A) Autoreactivity of supernatants from selected dual-κ (black bars) and single-κ (white bars) LPS-induced IgM$^+$ B cell hybridomas. Supernatants were tested for reactivity against chromatin (left), Smith antigen (middle), and HEp-2 cells (right). Anti-chromatin and anti-Smith ODs at 405 nm were normalized for total IgM as described in Materials and methods. In both assays, the supernatant of a 3-83-IgM–secreting B cell clone (specific for MHC I H-2K^{b,k}; Ozato et al., 1980) was used as negative control (gray bars, representing mean OD and SD, $n = 14$). Reactivity of supernatants with Hep-2 cells was measured by indirect immunofluorescence as described in Materials and methods. The supernatant of a B1-8-IgM–secreting B cell clone (specific for NP; Reth et al., 1978) was used as negative control (gray bar, representing mean intensity and SD, $n = 14$). The cutoff for positivity in each assay was set to three times the SD of the negative control, as represented by the dashed line. Hybridomas were classified as autoreactive when their supernatant generated signals above the dashed line. This analysis is representative of 14 independent experiments with a total combined of $n = 151$ hybridomas tested (see Table 2). (B) Dual-κ and single-κ B220$^+$CD19$^+$CD11b$^-$ B cells were sorted from mixtures of spleen and LN cells isolated from three MRL/*lpr-lgk*$^{m/h}$ mice of 14 (top), 17 (middle), and 29 (bottom) weeks of age, respectively, and cultured in equal numbers for 7 d with or without a TLR7 agonist. Graphs represent the titers of anti-chromatin and anti-Smith IgG (left and middle) and the integrated intensity for HEp-2 reactivity (right) obtained with supernatants collected from dual-κ (black bars) and single-κ (white bars) cell cultures. The analysis of the 14-wk-old mouse cells is representative of two independent analyses. The analysis of the 17 and 29-wk-old mice was performed once, but the sample of the 29-wk-old mouse was independently tested two times with similar results.

Table 2. Analysis of autoreactivity of LPS-induced B cell hybridomas from CB17-*Igk*$^{m/h}$ and MRL/*lpr*-*Igk*$^{m/h}$ mice

Self-reactivity	MRL/*lpr*		CB17	
	κ/κ	κ	κ/κ	κ
Chromatin	38%	11%	30%	12%
Smith	19%	19%	21%	12%
Hep2	38%	27%	51%	18%
Overall Autoreactive	72%	46%	60%	33%
Total tested	21	34	47	49

These hybridomas were randomly selected among those described in Table 1. All hybridoma were IgM except two that were IgG.

spleen and LN cells of three individual MRL/*lpr*-*Igk*$^{m/h}$ mice and screened them for the expression of mκ, hκ, and λ by flow cytometry and ELISA. Surprisingly, ∼80% of all hybridomas from all three mice represented an identical dual-κ/λ B cell clone bearing germline V_H7-*3*-D_H1-*1*-J_H2, V_k6-*17*-J_k4, and *Vλ 1*-*Jλ 1* genes and expressing IgM antibodies reactive to Smith antigen (Table 3 and not depicted). Given that κ/λ cells are rare in MRL/*lpr*-*Igk*$^{m/h}$ mice, the frequent representation of this clone suggests that these Smith-reactive IgM$^+$ B cells were highly prone to fuse with the myeloma cell line. In addition to the κ/λ clone, we identified an LN-derived dual-κ clone bearing somatically mutated V_H1-*7*-D_H2-*3*-J_H3 and V_k12-*46*-J_k1 genes and a germline encoded V_k2-*137*-J_k4 gene and expressing IgG antibodies reacting with chromatin (Table 3). Overall, results from the hybridoma analyses indicate that the population of dual-κ B cells comprises a higher frequency of autoreactive clones than that of single-κ B cells in both autoimmune and nonautoimmune mice, and that dual–L chain autoreactive B cells can be selected into the in vivo–activated cell pool of MRL/*lpr* mice.

MRL/*lpr* dual-κ B cells secrete IgG autoantibodies in response to TLR7 stimulation

To determine the propensity of dual-κ B cells to generate IgG switched autoantibodies relative to single-κ B cells, we sorted single- and dual-κ B220$^+$CD19$^+$ B cells (and excluding the CD11b$^+$ cell subset; Rubtsov et al., 2011) from MRL/*lpr*-*Igk*$^{m/h}$ mice of 14, 17, and 29 wk of age. Sorted cells were cultured with and without TLR7 stimulation, and their supernatant was analyzed for reactivity against chromatin, Smith, and HEp-2. The production of IgG autoantibodies was increased upon TLR7 stimulation of both single- and dual-κ B cells but was significantly higher in dual-κ B cells in all mice analyzed and, therefore, irrespective of age (Fig. 5 B). These data indicate that dual-κ B cells have a higher propensity to generate IgG autoantibodies than single-κ B cells in MRL/*lpr* mice at both early and late stages of disease.

Dual-κ B cells are highly selected into the plasmablast and memory B cell populations in MRL/*lpr* mice where they are partly regulated by Fas

Upon appropriate stimulation, B cells undergo blast formation and proliferation. A fraction of these activated B cells differentiate into plasmablasts, which are proliferating antibody-secreting cells with cell surface markers similar to those of plasma cells (PCs) but that retain detectable levels of surface Ig (Calame, 2001; William et al., 2005; Oracki et al., 2010). Activated B cells can also differentiate into strictly antibody-secreting PCs, but rheumatoid factor–producing B cells have been shown to differentiate mostly into plasmablasts in MRL/*lpr* mice (William et al., 2005).

To determine the ability of dual-κ B cells to differentiate into plasmablasts and PCs, we analyzed spleen and LN cells for the expression of B220, CD138, and CD44 together with surface and/or cytoplasmic Igκ and defined three stages of differentiation (Fig. 6 A): early plasmablast (B220$^+$CD138$^+$CD44^{high}

Table 3. Dual L-chain spontaneous hybridomas from MRL/*lpr*-*Igk*$^{m/h}$ mice

Hybridoma	Isot.	React.	H chain[a]				L chain[a]		
			VH	DH	JH	CDR3	VL	JL	CDR3
Dual-κ/λ									
LN 2A4[b]	IgM	Sm	V_H7-3 (S107)	D_H1-1 (DFL16.1)	J_H2	CARYVTTVPNFDYW (gl)	Vκ6-17 (Vκ19/28)	Jκ4	CQQHYSTPFTF (gl)
							Vλ1	Jλ1	CALWYSNHWVF (gl)
Dual-κ/κ									
LN 2A8[c]	IgG	Chr	V_H1-7 (J558)	D_H2-3 (DSP2.9)	J_H3	CARGWLLRTYW (12 mut)	Vκ12-46 (Vκ12/13)	Jκ1	CQHFYGTPWTF (7 mut)
							Vκ2-137 (Vκ24/25)	Jκ4	CMQHLEYPFTF (gl)

These two hybridomas were among 816 spontaneous B cell hybridomas generated from nonmanipulated spleen and LN cells of three individual MRL/*lpr*-*Igk*$^{m/h}$ mice (a total of six fusions). Isot., isotype; React., reactivity; Sm, Smith antigen; Chr, chromatin; gl, germline sequence; mut, number of predicted somatic mutations in the overall V(D)J sequence based on comparison with IMGT-deposited germline sequences.

[a]Ig H and L chain gene segments are reported with the IMGT nomenclature. The old nomenclature is given in parenthesis under the IMGT nomenclature.

[b]This hybridoma is representative of many clones (∼80% of the all hybridomas) isolated from both the spleen and LNs in all fusions.

[c]This hybridoma was from the fusion of LN cells from one MRL/*lpr*-*Igk*$^{m/h}$ mouse.

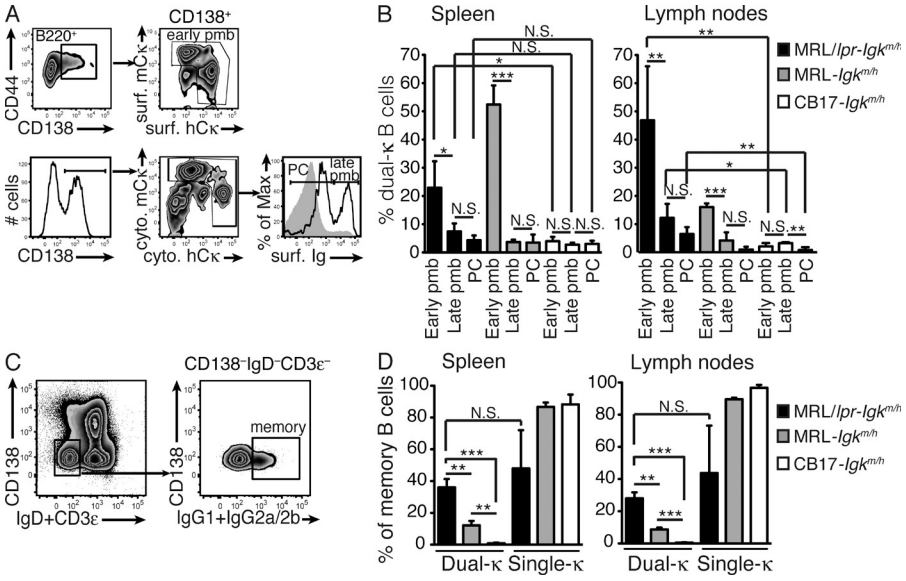

Figure 6. Dual-κ B cells are highly enriched in the plasmablast and memory B cell fractions of MRL/*lpr* mice and partly independent of Fas inactivation. (A) Zebra and histogram plots represent flow cytometric gating strategies applied to spleen cells isolated from one MRL/*lpr*-*Igk*$^{m/h}$ mouse. Early plasmablast (pmb) cells (top plots) were gated consecutively as B220$^+$, CD138$^+$CD44^{high}, and surface Igκ$^+$. Late pmb cells and PCs (bottom plots) were gated in succession as CD138$^+$, cytoplasmic Igκ^{high}, and then either surface Ig-positive (late pmb) or surface Ig-low/negative (PCs). Surface Igs were stained with a combination of anti-IgM, IgG1, and IgG2a/2b antibodies. The shaded gray histogram in the bottom right represents Igκ$^-$ non-B cells to depict a control surface Ig-negative cell population. This analysis is representative of three independent experiments. (B) Bar graphs represent mean frequency ± SD of dual-κ cells within early pmb, late pmb, and PC populations (gated as in A) in spleen and LNs of MRL/*lpr*-*Igk*$^{m/h}$ (black bars), MRL-*Igk*$^{m/h}$ (gray bars), and CB17-*Igk*$^{m/h}$ (white bars) mice. Data are from three independent experiments, with a total combined of $n = 5$–6 mice per group. (C) Representative flow cytometric analysis of memory B cells gated first as CD138$^-$ (to exclude plasmablasts and PCs) and IgD$^-$CD3ε$^-$ (to exclude naive B cells and T cells), followed by gating on IgG$^+$ (IgG1 and IgG2a/2b) cells from one MRL/*lpr*-*Igk*$^{m/h}$ mouse. This analysis is representative of at least three independent experiments with a total combined of $n = 7$ mice per group. (D) Bar graphs represent mean frequency ± SD of dual-κ and single-κ B cells in the memory B cell population (gated as in C) in spleen and LNs of MRL/*lpr*-*Igk*$^{m/h}$ (black bars), MRL-*Igk*$^{m/h}$ (gray bars), and CB17-*Igk*$^{m/h}$ (white bars) mice. Data are from three independent experiments, with a total combined of $n = 4$–7 mice per group. In the whole figure, MRL/*lpr*-*Igk*$^{m/h}$ and CB17-*Igk*$^{m/h}$ mice were at 18 wk of age and MRL-*Igk*$^{m/h}$ mice were at 30 wk of age. ***, $P < 0.001$; **, $P < 0.01$; *, $P < 0.05$. N.S., not significant.

surface-Igκ$^+$), late plasmablast (CD138$^+$ cytoplasmic-Igκ^{high} surface-Igκ$^+$), and PC (CD138$^+$ cytoplasmic-Igκ^{high} surface-Igκ$^{-/low}$). The early and late plasmablast stages were defined based on preliminary analyses in which we observed CD138$^+$ surface-Ig$^+$ cells that were mainly either B220$^+$ cytoplasmic-Ig^{low} (early plasmablasts) or B220$^-$ cytoplasmic-Ig^{high} (late plasmablasts). Upon these analyses, we found that in 18-wk-old MRL/*lpr*-*Igk*$^{m/h}$ mice, 20–50% of early plasmablasts were dual-κ cells (Fig. 6 B), a frequency 5–10-fold higher than in the naive mature B cell population of the same mice and of the plasmablast population of CB17-*Igk*$^{m/h}$ mice. Moreover, we found a similar enrichment of dual-κ B cells in the plasmablast population of 30-wk-old Fas-sufficient MRL-*Igk*$^{m/h}$ mice (Fig. 6 B), indicating that the MRL genetic background alone drives significant plasmablast differentiation of dual-reactive B cells. In the late plasmablast and PC subsets of MRL-*Igk*$^{m/h}$ and MRL/*lpr*-*Igk*$^{m/h}$ mice, the frequency of dual-κ cells was reduced from the early plasmablast stage (Fig. 6 B), suggesting that not all dual-κ plasmablasts are selected for entry into the nondividing PC population. Nevertheless, in the LNs the percentages of dual-κ cells in the late plasmablast and PC populations of MRL/*lpr*-*Igk*$^{m/h}$ mice were still above those seen in the same populations of CB17-*Igk*$^{m/h}$ mice (Fig. 6 B).

Antigen-activated B cells can alternatively differentiate into memory B cells. To examine this pathway of differentiation, we measured the frequency of dual-κ B cells in the IgG$^+$ cell subset in spleen and LNs of the same autoimmune and nonautoimmune mice (Fig. 6 C). The frequency of dual-κ B cells in the IgG$^+$ memory B cell population of CB17-*Igk*$^{m/h}$ mice was 1–3%, similar to that previously described (Casellas et al., 2007). This frequency was markedly increased in autoimmune MRL/*lpr*-*Igk*$^{m/h}$ mice where up to 40% of the Ig switched memory B cells were dual-κ cells (Fig. 6 D). Recent studies have indicated that the survival of IgG$^+$ autoreactive B cells in MRL/*lpr* mice is synergistically mediated by the *Fas*^{lpr} allele and the *MRL* genes (Aït-Azzouzene et al., 2010). Similarly, the frequency of dual-κ B cells in the IgG$^+$ B cell population of Fas-sufficient MRL-*Igk*$^{m/h}$ mice was intermediate between that of Fas-deficient MRL/*lpr* mice and nonautoimmune CB17 mice (Fig. 6 D). Our findings, therefore, indicate that approximately half of the IgG switched dual-κ B cells are eliminated via Fas-mediated cell death. These data indicate that the autoimmune-prone MRL genetic background drives significant selection of dual-κ mature B cells into the plasmablast and memory B cell populations, and that maintenance of dual-κ memory B cells is partly dependent on the inactivation of Fas.

Dual-κ B cells of autoimmune mice display increased frequency of activation and differentiation into plasmablasts that secrete autoantibodies

The increased selection of dual-κ B cells into the plasmablast and memory subsets of autoimmune mice suggests that dual-κ cells are more prone to activation than single-κ cells in the context of autoimmunity. To provide support to this hypothesis,

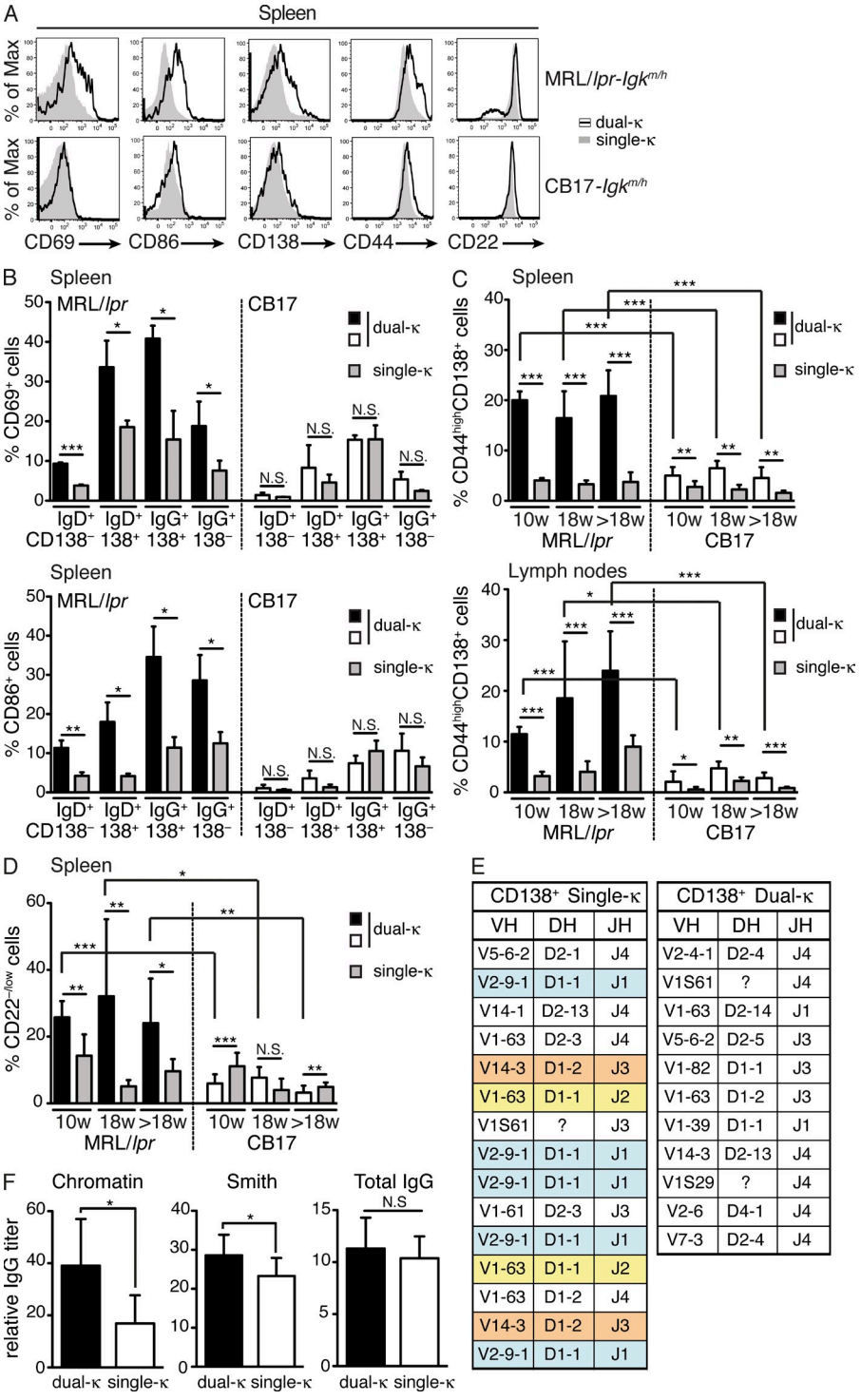

CD138+ Single-κ		
VH	DH	JH
V5-6-2	D2-1	J4
V2-9-1	D1-1	J1
V14-1	D2-13	J4
V1-63	D2-3	J4
V14-3	D1-2	J3
V1-63	D1-1	J2
V1S61	?	J3
V2-9-1	D1-1	J1
V2-9-1	D1-1	J1
V1-61	D2-3	J3
V2-9-1	D1-1	J1
V1-63	D1-1	J2
V1-63	D1-2	J4
V14-3	D1-2	J3
V2-9-1	D1-1	J1

CD138+ Dual-κ		
VH	DH	JH
V2-4-1	D2-4	J4
V1S61	?	J4
V1-63	D2-14	J1
V5-6-2	D2-5	J3
V1-82	D1-1	J3
V1-63	D1-2	J3
V1-39	D1-1	J1
V14-3	D2-13	J4
V1S29	?	J4
V2-6	D4-1	J4
V7-3	D2-4	J4

Figure 7. Dual-κ B cells of autoimmune mice display increased frequency of activation and differentiation into plasmablasts that secrete autoantibodies. (A) Histograms represent expression of CD69, CD86, CD138, CD44, and CD22 on live single B220+ dual-κ (solid line) and single-κ (shaded gray) B cell populations in the spleen of MRL/*lpr*-*Igk*$^{m/h}$ (top row) and CB17-*Igk*$^{m/h}$ (bottom row) mice. These analyses are representative of at least two independent experiments. (B) Bar graphs represent mean frequency ± SD of CD69+ (top) and CD86+ (bottom) cells in dual-κ (black and white bars) and single-κ (gray bars) B cell populations of spleen in MRL/*lpr*-*Igk*$^{m/h}$ (left) and CB17-*Igk*$^{m/h}$ (right) mice at 14–15 wk of age. Data are from two independent experiments with a total combined of $n = 4$ mice per group. (C and D) Bar graphs represent mean frequency ± SD of CD44^{high}CD138+ cells (C) and CD22^{low} cells (D) in dual-κ (black and white bars) and single-κ (gray bars) B cell populations of spleen (C and D) and LNs (only in C) in MRL/*lpr*-*Igk*$^{m/h}$ (left) and CB17-*Igk*$^{m/h}$ (right) mice at the age indicated on the x-axis. Data are from at least three independent experiments with a total combined of $n = 6$ mice per each age group. (E) Analysis of Ig $V_HD_HJ_H$ sequences from CD138+ single and dual-κ B cells. cDNA was generated from CD138+ single or dual-κ-positive cell populations sorted from one 15-wk-old MRL/*lpr*-*Igk*$^{m/h}$ mouse. IgH VDJ sequences were amplified and cloned as described in Methods. 15 and 11 clones from single-κ (left table) and dual-κ (right table) cell populations, respectively, were randomly selected for sequencing and each sequence was assigned to a VH, DH, and JH gene segment according to the IMGT website. Sequences that repeated more than once are highlighted in color. The clone sequences were obtained over the course of two independent experiments. (F) Analysis of antibodies secreted by plasmablasts. Dual-κ and single-κ CD138+ plasmablasts were sorted from mixtures of spleen and LN cells isolated from individual MRL/*lpr*-*Igk*$^{m/h}$ mice of 14–15 wk of age and cultured in equal numbers for 7 d without stimulation. Graphs represent the mean relative IgG titers + SD ($n = 3$) of anti-chromatin antibodies (left), anti-Smith antibodies (middle), and total IgG (right) in the supernatants of dual-κ (black bars) and single-κ (white bars) cell cultures. The cells were sorted and cultured from three individual MRL/*lpr*-*Igk*$^{m/h}$ mice on different days, and the supernatants were frozen and then analyzed by ELISA on the same day to reduce intra-experimental variability. ***, $P < 0.001$; **, $P < 0.01$; *, $P < 0.05$. N.S., not significant.

we analyzed the expression of the two general lymphocyte activation markers, CD69 and CD86 (Fig. 7 A), on single- and dual-κ B cells that belong to B cell subsets prior and after antigen selection. Specifically, we analyzed the activation state of B cells in preplasmablast (IgD+CD138−), nonswitched plasmablast (IgD+CD138+), switched plasmablast (IgG+CD138+), and memory (IgG+CD138−) B cell subsets in spleen (Fig. 7 B) and LNs (not depicted). The frequency of activated dual-κ

B cells in the spleen of 14–15-wk-old MRL/*lpr-Igk*$^{m/h}$ mice was significantly higher than that of single-κ B cells in the same mice and when compared with single- and dual-κ B cells in CB17-*Igk*$^{m/h}$ mice (Fig. 7 B). Moreover, MRL/*lpr-Igk*$^{m/h}$ dual-κ B cells were found to be more frequently activated in all B cell subsets analyzed and, thus, before and after a putative antigen selection event (Fig. 7 B). Similar results were observed in LNs (unpublished data).

To extend these findings, we next analyzed the expression of the plasmablast differentiation markers CD138, CD44, and CD22. The dual-κ B cell population in spleen (Fig. 7 A) and LNs (not depicted) of MRL/*lpr-Igk*$^{m/h}$ mice displayed higher levels of CD44 and CD138 and lower levels of CD22 compared with the single-κ B cell population. In contrast, the expression profile of these markers appeared identical in the single and dual-κ B cell populations of CB17-*Igk*$^{m/h}$ mice (Fig. 7 A). The frequency of CD44^{high}CD138^{+} cells and of CD22^{low} cells in the dual-κ subset of spleen and LNs of MRL/*lpr-Igk*$^{m/h}$ mice was twice that seen in the single-κ subset in the same mice (Fig. 7, C and D; and not depicted). This difference was already present at 10 wk of age and increased with the age of the mice in the LNs. Although in most MRL/*lpr* mice ∼20% of the dual-κ B cells appeared to be plasmablasts, in healthy mice only ∼5% of single and dual-κ B cells displayed this phenotype (Fig. 7, C and D). These findings indicate that dual-κ B cells have a higher propensity to be activated and to differentiate into plasmablasts in autoimmune mice.

We next asked whether the selection of dual-κ B cells into the plasmablast population of autoimmune mice is a general feature of these cells or if it only occurs in a small subset of cells. If dual-κ B cells have a general selection advantage for activation, we expect the plasmablast pool to contain a diverse repertoire instead of an oligoclonal expansion. To address this question, we performed a limited study where we amplified and cloned the variable region of the *Igh* chain gene from a sorted pool of CD138^{+} dual-κ and single-κ MRL/*lpr-Igk*$^{m/h}$ B cells and sequenced 11–15 randomly selected clones. Each of the 11 VDJ sequences cloned from CD138^{+} dual-κ cells was unique, whereas only 9 of the 15 sequences from single-κ cells were diverse (Fig. 7 E). This suggests that dual-κ B cells are generally selected into the plasmablast subset, and not via the preferential expansion of few clones.

As shown by the LPS-induced hybridoma analysis, most dual-κ B cells express autoantibodies. Therefore, we next asked whether dual-κ B cells selected into the plasmablast subset are also autoreactive. To address this question, we sorted CD138^{+} single and dual-κ B cells from three individual 14–15-wk-old MRL/*lpr-Igk*$^{m/h}$ mice and cultured the same number of cells for 7 d without stimulation. Total IgG and IgG specific for chromatin and Smith were measured in the cell supernatants. Both single- and dual-κ CD138^{+} cells secreted anti-chromatin and anti-Smith IgG antibodies (Fig. 7 F). However, dual-κ CD138^{+} cells secreted significantly more IgG autoantibodies when compared with single-κ cells, whereas total IgG was similar (Fig. 7 F). These data indicate that dual-κ autoreactive B cells are selected into the plasmablast population retaining the capacity to secrete IgG autoantibodies.

DISCUSSION

Although allelic and isotypic exclusion are strongly enforced during B cell development, a small number of B cells develop coexpressing more than one type of Ig H or L chain (Nossal and Makela, 1962; Pauza et al., 1993; Giachino et al., 1995; Li et al., 2001; Gerdes and Wabl, 2004; Rezanka et al., 2005; Casellas et al., 2007; Velez et al., 2007; Kalinina et al., 2011) and are capable of IgG class switch recombination and antibody production in healthy mice and people (Giachino et al., 1995; Casellas et al., 2007; Velez et al., 2007). Here, we show that in autoimmune mice with a wild-type polyclonal Ig repertoire, dual-κ B cells are generated at higher numbers than in healthy mice, they are self-reactive more frequently than single-κ B cells, and they are highly enriched in the antigen-selected B cell subsets.

Within the polyclonal Ig repertoire of healthy mice, dual-κ B cells have been demonstrated to arise after receptor editing in autoreactive immature B cells (Casellas et al., 2007). In these previous studies, dual-κ immature B cells were delayed in development relative to single-κ B cells and this delay was suggested to be caused by the receptor editing process. In our studies however, we found that dual-κ immature B cells have kinetics of development that are faster than single-κ B cells in MRL/*lpr* mice, thus exhibiting a behavior different than that of developing dual-κ B cells in healthy mice (Casellas et al., 2007; and our results). We argue that this difference might be a result of the reduced efficiency of the receptor editing process that has been documented in MRL/*lpr* mice (Li et al., 2002a; Lamoureux et al., 2007; Panigrahi et al., 2008). Specifically, we propose that autoreactive immature B cells in MRL/*lpr* mice might undergo a round of receptor editing resulting in the expression of a nonautoreactive κ chain, but that the editing process is aborted before its completion and the inactivation of the *Vκ* gene encoding the autoreactive chain. This hypothesis also implies that single-κ immature B cells undergo a more extensive editing process than dual-κ B cells in MRL/*lpr* mice. An alternative explanation would take into account the possibility that developing MRL/*lpr* B cells exhibit defects in the control of light chain allelic exclusion, whereby both *Igk* alleles rearrange simultaneously without delaying the maturation of dual-κ B cells. Defects in allelic exclusion have been previously described in MRL/*lpr* mice (Roark et al., 1995b). Furthermore, our results do not exclude the possibility that the increased frequency of dual-κ immature B cells in MRL/*lpr* mice might be caused by increased cell proliferation which, although unusual at this stage of cell differentiation, would be also compatible with the higher BrdU incorporation rates. The increased positive selection of dual-κ autoreactive immature B cells into the peripheral compartment of MRL/*lpr* mice would nevertheless require an intrinsic higher threshold for tolerance induction, a feature supported

by previous studies (Roark et al., 1995a; Mandik-Nayak et al., 1999). Moreover, we have recently demonstrated that positive selection of immature B cells into the peripheral compartment is an active process depending on the combined activities of tonic BCR and BAFFR signaling (Rowland et al., 2010a,b). Thus, we envision that the increased generation of dual-reactive B cells in MRL/*lpr* mice might also be the result of an improved efficiency of these positive selective events led by the coexpression and signaling of nonautoreactive BCRs. We also note that the frequency of $BrdU^+$ cells among the transitional B cells in the BM of MRL/*lpr* mice was higher than that of immature B cells, suggesting an unusual proliferation burst of those cells in this particular mouse strain. This proliferation event could further contribute to the enhanced generation of dual-κ cells in the periphery of autoimmune mice. Overall, we speculate that a reduced threshold for negative selection, inefficient levels of receptor editing and allelic exclusion, an improved efficiency of positive selection, and/or an aberrant cell proliferation event can promote higher generation of dual-κ chain B cells in MRL/*lpr* mice. Further studies are required to find out which of these mechanisms play the major role in the generation of dual-reactive B cells in autoimmune mice. Our observation that dual-κ B cells are also generated more frequently in MRL mice indicates that this process is independent of the function of Fas.

We further observed that the generation of dual-κ B cells increased after 10 wk of age in MRL/*lpr* mice, at a time when autoantibody titers and disease become more significant. Although these findings support the idea that dual-κ B cells play a role in autoantibody formation and disease progression, they also suggest that some element of autoimmunity might exacerbate the potential defects in early B cell development and tolerance discussed here, enhancing the generation of autoreactive dual-κ chain B cells. This feedback might be mediated by autoantibodies that increase with disease progression. Autoantibodies that are made within, or that circulate to, the BM can bind to local self-antigens potentially masking these antigens from B cells and consequently reducing levels of antigen-mediated BCR signals. An opposite phenomenon mediated by circulating antibodies and affecting tolerance induction of rheumatoid factor B cells has been previously described (Wang and Shlomchik, 1998).

Despite increased generation and/or selection of dual-κ B cells in the BM of MRL/*lpr* mice, our data demonstrate that a fraction of these cells never reach the splenic FO B cell compartment, indicating that they might be targeted by negative selection at the early transitional B cell stage or otherwise differentiate into a different mature cell subset (i.e., the MZ). Of note, half of the dual-κ B cells in the late transitional population were found in the T3 subset and, therefore, might be anergic cells blocked in differentiation (Merrell et al., 2006).

Previous studies have shown that the MRL/*lpr* genetic background precludes the recruitment of anti-DNA dual-κ/λ B cells into the MZ cell population and suggested that these mice are unable to sequester autoreactive B cells in this subset (Li et al., 2002b). We found, however, that dual-κ B cells localize more frequently in the MZ B cell pool than in the FO B cell subset in MRL mice and independent of the function of Fas. These contrasting observations suggest that the presence of dual-reactive B cells in the MZ or FO B cell subsets might depend on their level of autoreactivity or type of specificity, as previously elegantly demonstrated with the anti–Thy-1 mouse model (Wen et al., 2005). Alternatively, the reduced frequency of anti-DNA κ/λ B cells observed in previous studies might be the result of reduced receptor editing during B cell development. We noticed that dual-κ/λ B cells are not frequently generated in MRL/*lpr* mice. This further supports the idea that receptor editing often aborts early and before reaching the stage of *Igλ* gene recombination in these mice, with the consequence of a general reduced frequency of dual-κ/λ B cells.

The frequency of dual-κ B cells was increased from 3–10% in the naive mature B cell population to 20–50% (i.e., 5–10-fold) in the early plasmablast subset in autoimmune mice, whereas it remained unchanged in nonautoimmune mice. The enrichment of dual-κ plasmablasts was also observed in MRL mice indicating that it does not require defects in the Fas pathway. The high frequency of dual-κ B cells in the plasmablast population suggests that dual-κ mature B cell undergo increased activation and subsequent selection into the plasmablast subset relative to single-κ B cells. In support of this model, we found that the fraction of activated ($CD69^+$ and $CD86^+$) cells in the naive (IgD^+CD138^-) B cell population was significantly higher in the dual-κ subset relative to the single-κ subset of autoimmune mice. In spite of this, we isolated only one dual-κ spontaneous B cell hybridoma from six fusions (spleen and LNs) performed with cells from three MRL/*lpr* mice. We propose that this apparent discrepancy between our flow cytometric and hybridoma analyses reflects an experimental feature by which certain clones are particularly activated in vivo, fuse more readily, and quickly outgrow other clones. In fact, our spontaneous hybridoma collection was dominated by a κ/λ Smith-reactive clone despite the fact that κ/λ cells were never >1% of all B cells in vivo (unpublished data). It is unclear why this κ/λ clone was so prevalent in our spontaneous hybridoma collection when such oligoclonality has not been previously reported by others. The possibility that this κ/λ clone was a contaminant in our cultures is negligible because fusions from two mice were done several weeks apart from those of the first mouse and this clone was only observed in the spontaneous fusions from MRL/*lpr* mice among the many B cell fusions performed in our laboratory in the same period of time. The prevalence of this κ/λ clone might be a result of our hybridoma methodology that may select for fast growing clones or to the specific MRL/*lpr* strain that was bred in our colony.

Distinct mechanisms can lead to the generation of plasmablasts, and not all require specific antigen recognition by the BCR. Plasmablast differentiation can follow polyvalent antigen-mediated stimulation of B1 and MZ B cells, the combined antigen and T cell help–mediated activation of FO B cells, or the TLR-mediated polyclonal activation of mature

and memory B cells. Our studies do not discriminate between these mechanisms. However, we observed a significantly higher frequency of activated dual-κ than single-κ B cells at stages of mature B cell differentiation before and after plasmablast formation in MRL/*lpr* mice. This finding suggests that dual-κ B cells are more prone to activation, whether by antigen or by nonantigenic stimuli. Additionally, the frequent observation of dual-κ cells within the IgG^+ memory B cell subset of autoimmune mice suggests that at least some of the dual-κ mature B cells are positively selected after antigen binding and with the additional support of T cell help. In autoimmune-prone mice, positive selection of B cells can be mediated by either self- or foreign antigens. The enhanced positive selection of dual-κ B cells into the plasmablast and memory cell subsets might be simply a result of the higher prevalence of self-reactivity in the dual-κ B cell population, which was demonstrated by both the analyses of LPS-induced hybridomas and of ex vivo cells. However, the coexpression of a nonautoreactive BCR in this context might also play a role in the selection of dual-κ B cells, either by mediating a prosurvival tonic BCR signal (Lam et al., 1997) or by engaging foreign antigen. Further studies are required to test these hypotheses.

Burnet postulated that for optimal negative selection of self-reactivities and positive selection and expansion of foreign reactivities, antibody-producing cells are predetermined for the expression of specificities reactive with only one antigenic determinant (Burnet, 1959). Our findings partially support Burnet's theory by showing that negative selection of B cells is compromised by dual-reactivity, whereas positive selection is not affected in healthy conditions and enhanced in autoimmunity. The important question, however, is whether dual-reactive B cells play an active role in the development of autoimmunity. Results from our studies, although not resolving this issue, provide support to the idea that dual-κ B cells significantly contribute to the IgG autoantibody pool of autoimmune MRL/*lpr* mice. We based this conclusion on the following observations. First, when stimulated with a TLR-7 agonist, dual-κ B cells secrete IgG autoantibodies in greater amounts than single-κ B cells. Second, dual-κ B cells represent up to half of the plasmablasts and IgG memory B cells in autoimmune mice, cell populations which have been shown to significantly contribute to autoimmunity (William et al., 2005; Herlands et al., 2007). Third, $CD138^+$ dual-κ plasmablasts secrete IgG autoantibodies in greater amounts than $CD138^+$ single-κ cells and in the absence of stimulation. Whether the autoantibody made by dual-κ B cells is of pathogenic quality is not yet clear, and this question will require evaluation of the somatic mutations in Ig genes of IgG^+ plasmablasts and of the affinity for self-antigens of their antibody products. Our finding of a spontaneous MRL/*lpr* dual-κ B cell hybridoma that expresses mutated IgG anti-chromatin autoantibodies would indicate that autoreactive dual-κ B cells are capable of undergoing somatic hypermutation and positive selection in the germinal center or in extra-FO foci (Herlands et al., 2007, 2008; Odegard et al., 2008; Rankin et al., 2012). Our data further suggest that at least half of the IgG^+ memory B cells that arise in MRL/*lpr* mice develop as a result of aberrant Fas signaling, as evidenced by the fact that their frequency was diminished in Fas-sufficient MRL mice, and in agreement with recent elegant studies on the selection of autoreactive IgG^+ B cells (Aït-Azzouzene et al., 2010). It is interesting, moreover, that dual-κ B cells were mostly found in the plasmablast population, an observation similar to that made in rheumatoid factor–expressing mice in which the plasmablasts are the major source of autoantibodies (William et al., 2005; Herlands et al., 2007).

Although MRL/*lpr* and MRL mice do not precisely reflect systemic lupus erythematosus (SLE) in humans, many of the features of this autoimmune disease are recapitulated in these mouse models. Our findings on dual-reactive B cells in the autoimmune mouse strains lead us to consider that these B cells may also be a feature of SLE in humans and partly independent of defects in the Fas pathway, a possibility which will be tested in future studies. B cells are essential for the development of autoimmunity in both MRL and MRL/*lpr* mice (Chan and Shlomchik, 1998; Chan et al., 1999; Li et al., 2008). Results from our studies in lupus-prone mice indicate that dual-reactive B cells are generated more frequently with autoimmunity, they are more often autoreactive, they are a major component of the plasmablast and memory B cell subsets, and they contribute to the pool of IgG autoantibodies. Our findings, therefore, suggest that dual-reactive B cells might play a part in the development and/or exacerbation of this disease.

MATERIALS AND METHODS

Mice $Igk^{m/h}$ mice have been previously described (Casellas et al., 2001; Velez et al., 2007). These mice that were initially on a mixed (129xC57BL/6) genetic background were backcrossed to CB17 for two generations and are referred here to as CB17-$Igk^{m/h}$ for simplicity. CB17-$Igk^{m/h}$ mice were backcrossed to MRL/*lpr* (MRL/MpJ-Fas^{lpr}/J) mice for 10 generations to generate MRL/*lpr*-$Igk^{m/h}$ mice. Every generation was analyzed by flow cytometry of peripheral blood cells for the presence of the Igk^h allele before selection of next generation breeders. Mice of the last generation were genotyped at the *Fas* allele (according to The Jackson Laboratory protocol) to select animals homozygous for the Fas^{lpr} mutation. MRL/*lpr*-$Igk^{h/h}$ mice were bred to MRL (MRL/MpJ) mice to generate MRL-$Fas^{lpr/+}$ $Igk^{m/h}$ mice (referred to as MRL-$Igk^{m/h}$). Both males and females of 6–30 wk of age were used in this study. All mice used for these studies were bred in house and maintained in specific pathogen–free rooms at the Biological Resource Center at National Jewish Health (NJH). All animal experiments were approved by the NJH Institutional Animal Care and Use Committee.

Cell preparation Single-cell suspensions from BM, spleen, and LNs were prepared in DME supplemented with 3% FBS. BM and spleen cells were treated with buffer with 0.15 M NH_4Cl, 10 mM $KHCO_3$, and 0.1 mM EDTA, pH 8.0, for 2 min to remove erythrocytes and washed by centrifugation in PBS supplemented with 3% FBS.

Antibodies and flow cytometric analysis Single-cell suspensions were first incubated with a rat anti–mouse FcγRII/III blocking antibody (2.4G2) for 15 min on ice to prevent unspecific binding of staining antibodies on cells through their Fc portion. Cells were then incubated for 20 min on ice with antibodies against surface markers. Fluorescent monoclonal antibodies against B220 (RA3-6B2), CD1d (1B1), CD138 (281–2), CD23 (B3B4), CD24

(M1/69), CD22 (OX-97), CD21 (eBio4E3), CD3e (145-2C11), CD44 (1M7), IgG1 (A85-1), IgG2a/2b (R2-40), IgD (11-26c-2a), CD19 (1D3), CD11b (M1/70), CD69 (H1.2F3), and CD86 (GL-1) were purchased from BD, BioLegend, or eBioscience, whereas those against IgM were either generated in house (R33-24.12) or purchased from Jackson ImmunoResearch Laboratories. Fluorescent or biotinylated polyclonal antibodies for Ig staining were a goat Fab' anti–human Igκ (Protos Immunoresearch), a goat anti–mouse (GAM) Igλ (SouthernBiotech), and a rat Fab anti–mouse Igκ (187.1, generated in house). To generate biotin-conjugated rat Fab anti–mouse Igκ antibodies, 187.1 IgG was first biotinylated using EZ-Link Sulfo-NHS-LC-Biotin (Thermo Fisher Scientific) and, subsequently, fragmented with papain. Briefly, equal volumes of 1 mg/ml 187.1 IgG-biot and 0.075 mg/ml papain (Papain 2× recrystallized suspension; Sigma Aldrich) diluted in digestion buffer (PBS, 0.02 M EDTA, and 0.02 M L-Cysteine) were mixed and incubated for 4 h at 37°C. The reaction was stopped by adding iodoacetamine (Sigma-Aldrich) at a 0.03 M final concentration. The mix was dialyzed against 1 liter of PBS overnight at 4°C, and Fc fragments and whole IgG were eliminated over a protein G column. The purity of Fab 187.1 was verified by Coomassie Blue coloration of SDS-PAGE gel in reducing and nonreducing conditions and by its inability to promote calcium influx in mouse B cells. Biotinylated antibodies were revealed with fluorochrome-conjugated streptavidin (either BD or eBioscience). 7-amino-actinomycin D (7AAD; BD) was added to some cell samples at 0.25 μg/10^6 cells to exclude dead cells from the analysis. Flow cytometric analysis was performed on live lymphocytes based on 7AAD staining and/or forward and side scatter using a LSRII cytometer (BD) and FlowJo software (Tree Star). Cell aggregates were excluded from the analysis by using a pulse area versus width gating (doublet discriminator channel).

Immunofluorescence histology Spleens and LNs were harvested from mice and frozen in Tissue-Tek OCT compound (Sakura) at −80°C. Using a cryostat, tissues were cut into 5–7-μm-thick sections and dried at room temperature for 20 min. Dried tissue sections were rehydrated in PBS for 20 min and blocked for 30 min with a mix of rat anti–mouse FcγRII/III blocking antibody 2.4G2, purified mouse IgG1 (Southern Biotech), and 3% goat serum (Gibco) in PBS at room temperature. Sections were stained with a mix of rat Fab anti–mouse Igκ-APC and goat Fab' anti–human Igκ-PE in PBS for 45–60 min at room temperature in the dark, and washed 3 × 5 min each in PBS shaking baths. Stained sections were dried, mounted with Fluoromount-G (Southern Biotech), and visualized with a microscope (Axiovert 200M; Carl Zeiss) using a 3i Marianas System (Intelligent Imaging Innovations) and SlideBook 4.0 software (Intelligent Imaging Innovations).

Sorting of dual-κ and single-κ B cells for in vitro analysis Dual-κ and single-κ B cells were sorted from either $B220^+CD19^+CD11b^-$ or $CD138^+$ cell fractions of spleen and LN cell mixtures using the anti-κ Fab antibody fragments described and after CD4 and CD8 T cell depletion. When incubated with B cells, these anti-κ antibodies did not trigger Ca^{++} influx in flow cytometric analyses. Cell sorting was performed using a MoFlo XDP (Beckman Coulter) and an ICyt Synergy cell sorter. Sorted cells were counted and cultured at 37°C for 7 d with or without 1 μg/ml of TLR7 agonist (R848; InvivoGen). Cell supernatants were collected and tested for reactivity against chromatin and Smith antigen by ELISA and for HEp-2 staining. The autoantibody titers in the supernatants were measured relative to a standard curve of a reference MRL/*lpr* serum diluted 200-fold and according to a method described in Fisher et al. (1988). Specifically, an equivalent dilution factor for each sample was calculated as 1 over the dilution value of the reference serum that gave an O.D. that was equivalent to that of the sample supernatant. These values were then multiplied by 10^3 to obtain whole numbers that were easier to graph (Fisher et al., 1988).

In vivo BrdU incorporation CB17-*Igk*$^{m/h}$ and MRL/*lpr*-*Igk*$^{m/h}$ mice were injected i.p. with 1 mg BrdU (Sigma-Aldrich) and then euthanized at 6, 12, or 24 h thereafter. For the 24-h time point, mice received a second BrdU injection at 12 h (Hippen et al., 2005; Casellas et al., 2007). BM cells were isolated from BrdU-treated and control untreated mice and stained for surface markers as described. Cells were then fixed and stained for BrdU using the APC BrdU Flow kit (BD) according to the manufacturer's protocol. Cytometric analysis was performed using an LSRII cytometer (BD) and FlowJo software.

Generation of B cell hybridomas and hybridoma supernatants LPS-induced and spontaneous B cells hybridomas were generated from CB17-*Igk*$^{m/h}$ and MRL/*lpr*-*Igk*$^{m/h}$ mice as previously described (Harris et al., 1992; Liu et al., 2005; Velez et al., 2007). Intracellular staining for IgL (hCκ, mCκ, and Igλ) chains was performed as previously described (Velez et al., 2007). Hybridomas were cultured in complete RPMI 1640 medium with 5% FBS precleared of bovine IgG by passage over protein G. Hybridoma supernatants were concentrated 50–100-fold over Centricon Plus-70 100-kD cut-off filters (Ultracel; Millipore), and IgM, IgG, mIgκ, hIgκ, and mIgλ were quantified by ELISA. Supernatants were then adjusted to an IgM or IgG concentration of 30 μg/ml and tested for autoreactivity. Each hybridoma supernatant was analyzed by ELISA in duplicate and a mean OD_{405} was calculated. To normalize the antigen-specific reactivity in each hybridoma supernatant for the total Ig concentration, the ODs relative to the antigen-specific ELISAs were divided by the ODs relative to the isotype-specific (IgM or IgG) ELISAs for the same supernatant dilutions. These OD values were always within the linear part of the standard curves. The supernatant of a 3–83-IgM-secreting B cell clone (specific for MHC I H-$2K^{b,k}$; Ozato et al., 1980) was used as negative control. Clones were considered autoreactive when their reactivity toward self-antigen was three times above the SD of the negative control signal. Polyreactive hybridomas, which were those producing antibodies that bound to LPS in addition to each of the autoantigens tested, were <5% of the total hybridomas and were excluded from this study.

Quantification of secreted Igs and antigen-specific antibodies by ELISA IgM, IgG, mIgκ, hIgκ, and mIgλ were quantified by ELISA as previously described (Velez et al., 2007). Absorbance values were read at 405 nm with a VersaMax ELISA reader (Molecular Devices). The detection of hIgκ/mIgκ chimeric antibodies was performed by ELISA as previously described (Velez et al., 2007). Standard chimeric antibody used for quantification was obtained from the supernatant of a dual-κ hybridoma (8G12-IgM). For the detection of anti-chromatin and anti-Smith antibodies, 96-well Nunc-Immuno plates were coated with 10 μg/ml calf thymic chromatin (a gift of L. Wysocki's laboratory) in PBS, 1 mM EDTA, 0.05% $NaNa_3$ buffer or 1 μg/ml of calf thymic Smith antigen (Meridian Life Science) in PBS, 15 mM Na_2CO_3, 35 mM $NaHCO_3$, and 3.1 mM NaN_3 carbonate buffer, respectively, and incubated overnight at 4°C. Plates were washed once with PBS and 0.05% Tween 20. Anti-chromatin plates were blocked with EDTA-blocking buffer (PBS, 1% BSA, 1 mM EDTA, and 0.05% $NaNa_3$), whereas anti-Smith plates were blocked with BSA-blocking buffer (PBS, 1% BSA, and 0.05% $NaNa_3$) for at least 2 h at 37°C before washing and further processing. Sera, hybridoma supernatants, or cell culture supernatants were diluted in either EDTA-blocking buffer or BSA-blocking buffer and added to the first well of the plates. Then, threefold serial dilutions were made in the same buffer and plates were incubated for 2 h at 37°C. Plates were washed three times and specificity was revealed with either AP-conjugated GAM Ig (H+L) or AP-conjugated GAM IgG (SouthernBiotech). Quantification of the Ig titers after these ELISAs is described in the previous sections.

HEp-2 reactivity assay The HEp-2 reactivity assay was performed using the ANA kit Hep-2 antigen substrate 12-well slides (BION Enterprises) using a quantitative method previously described (Peterson et al., 2009), with the exception that slides were revealed either with Cy5-conjugated anti–mouse IgG + IgM (H+L) antibodies (Jackson ImmunoResearch Laboratories) or with Alexa Fluor 680–conjugated $F(ab')_2$ GAM IgG (H+L) antibodies (Invitrogen) both diluted to 15 μg/ml. The Odyssey Infrared Imaging System and software (LI-COR) were used to detect and quantify the fluorescence intensity emitted from each well. Each sample was normalized by dividing the average fluorescent signal of duplicate wells by the average signal intensity of the positive control wells included on each slide. The normalized signal was designated as the integrated intensity. The positive control antibody used

for assaying IgM$^+$ hybridomas was from 5B5 (an IgM$^+$ anti-chromatin hybridoma, a gift of L. Peterson), and the negative controls were B1-8μ (an IgM clone reactive with 4-Hydroxy-3-nitrophenylacetyl hapten [NP]; Reth et al., 1978) and supernatant from SP2/0(mIL-6), the myeloma fusion partner. The positive control antibody used for assaying sorted cell supernatants and IgG$^+$ hybridomas was from 3H9 (an IgG$^+$ anti-DNA clone, a gift of L. Wysocki), and cell culture medium was used as negative control.

Ig gene analysis RNA was isolated from hybridoma cell lines and sorted CD138$^+$ single and dual-κ cells by TRIzol (Invitrogen) according to the manufacturer's protocol. DNA contaminants were removed using Ambion DNA-free kit (Ambion). cDNA was synthesized with oligo dT using the SuperScript III First-Strand Synthesis for RT-PCR kit (Invitrogen) according to the manufacturer's protocol. Ig genes were amplified on cDNA by PCR using Platinum Taq DNA Polymerase High Fidelity (Invitrogen). *Igh*VDJ sequences were amplified with a forward degenerate V_H primer 5′-CTGCA**ACCGGT**GTACATTCCSAGGTSMARCTGSAGSAGTCWGG-3′ (based on Orlandi et al., 1989; Dattamajumdar et al., 1996) and a mix of reverse J_H primers for J_H1 5′-TGCGAA**GTCGAC**CCTGAGGAGACGGTGACCGTGG-3′, J_H2 5′-TGCGAA**GTCGAC**CCTGAGGAGACTGTGAGAGTGG-3′, J_H3 5′-TGCGAA**GTCGAC**CCTGCAGAGACAGTGACCAGAG-3′, and J_H4 5′-TGCGAA**GTCGAC**CCTGAGGAGACGGTGACTGAGG-3′. *Igk* VJ sequences were amplified with a mix of forward degenerate Vκ primers 5′-CTGCA**ACCGGT**GTACATTCCGACATYSWGMTSACHCARTCT-3′ (based on Orlandi et al., 1989; Dattamajumdar et al., 1996), 5′-CA**ACCGGT**-GTACATTCCSAAAHTRYTSTSACCCAGTCT-3′, and 5′-CTGCA**ACC-GGT**GTACATTCCGATGTYSWGMTSACHCARRCT-3′ and a mix of reverse Jκ primers for Jκ1 5′-GCCAC**CGTACG**TTTGATTTCCAGCT-TGGTG-3′, Jκ2 5′-GCCAC**CGTACG**TTTTATTTCCAGCTTGGTC-3′, Jκ4 5′-GCCAC**CGTACG**TTTTATTTCCAACTTTGTC-3′, and Jκ5 5′-GC-CAC**CGTACG**TTTCAGCTCCAGCTTGGTC-3′. *Igλ* VJ sequences were amplified with a mix of forward Vλ primers for Vλ1,2 5′-CTGCA**ACCG-GT**GTACATTCCCAGGCTGTTGTGACTCAG-3′ and VλX 5′-CTG-CA**ACCGGT**GTACATTCCCAACTTGTGCTCACTCAGT-3′ and a mix of reverse Jλ primers for Jλ1 5′-CTCCTCA**CTCGAG**GCTAGGACAGT-CAGTTTGGTTCC-3′ and Jλ2,3 5′-CTCCTCA**CTCGAG**GCTAGGA-CAGTGACCTTGGTTCC-3′. All forward primers prime at the beginning of framework region 1 in the respective V genes. The nucleotides in bold represent restriction sites for cloning into expression vectors not used in this study. PCR conditions consisted of an initial cycle at 94°C for 2 min, followed by 35 cycles at 94°C for 30 s, 58°C for the *Igh* and *Igk* or 62°C for *Igλ* for 30 s, and 68°C for 1 min, followed by one final cycle at 68°C for 10 min. PCR products were resolved on a 1% agarose gel, and products were purified using the QIAquick Gel Extraction kit (QIAGEN) and cloned into the pCR4 vector with the TOPO TA Cloning Kit (Invitrogen). Plasmid DNA was isolated using Miniprep Spin kit (QIAGEN) and the insert sequenced by Beckman Coulter Genomics. Ig gene sequences were analyzed using the International Immunogenetics Information System website (http://www.imgt.org/).

Statistical analysis Statistical significance was calculated with Prism software (GraphPad Software, Inc.) using two-tailed unpaired or paired Student's *t* test depending on the data analyzed, with equal variance using Welch's correction when variances were significantly different. Data are represented as arithmetic means ± SD.

We acknowledge Dr. Lisa Peterson (NJH) for the help and training in the HEp-2 staining and analysis of fluorescence intensity. We thank the NJH flow cytometry facility for cell sorting and flow cytometry analysis. We are grateful to Dr. T. Detanico in Dr. Wysocki laboratory (NJH) for providing calf chromatin, and to M. Schuster and M. Kelly (UCD) for their technical help. We greatly appreciate the advice and comments of all members of the Pelanda and Torres laboratories during this study and those of Dr. Lenny Dragone (NJH) on the manuscript. Finally, we wish to thank the mice for sacrificing their life for our study.

This work was partly supported by National Institutes of Health grants PO1 AI022295, RO1 AI052310, and RO1 AI052157 and the Viola Vestal Coulter Foundation.

The authors declare that they have no competing financial interests.

Submitted: 10 February 2012
Accepted: 30 July 2012

REFERENCES

Ait-Azzouzene, D., L. Verkoczy, J. Peters, A. Gavin, P. Skog, J.L. Vela, and D. Nemazee. 2005. An immunoglobulin Cκ-reactive single chain antibody fusion protein induces tolerance through receptor editing in a normal polyclonal immune system. *J. Exp. Med.* 201:817–828. http://dx.doi.org/10.1084/jem.20041854

Aït-Azzouzene, D., D.H. Kono, R. Gonzalez-Quintial, L.J. McHeyzer-Williams, M. Lim, D. Wickramarachchi, T. Gerdes, A.L. Gavin, P. Skog, M.G. McHeyzer-Williams, et al. 2010. Deletion of IgG-switched autoreactive B cells and defects in Fas(lpr) lupus mice. *J. Immunol.* 185:1015–1027. http://dx.doi.org/10.4049/jimmunol.1000698

Andrews, B.S., R.A. Eisenberg, A.N. Theofilopoulos, S. Izui, C.B. Wilson, P.J. McConahey, E.D. Murphy, J.B. Roths, and F.J. Dixon. 1978. Spontaneous murine lupus-like syndromes. Clinical and immunopathological manifestations in several strains. *J. Exp. Med.* 148:1198–1215. http://dx.doi.org/10.1084/jem.148.5.1198

Barreto, V., and A. Cumano. 2000. Frequency and characterization of phenotypic Ig heavy chain allelically included IgM-expressing B cells in mice. *J. Immunol.* 164:893–899.

Burnet, F.M. 1959. Clonal Selection Theory of Acquired Immunity. Cambridge University Press and Vanderbilt University Press, London and Nashville. 208 pp.

Calame, K.L. 2001. Plasma cells: finding new light at the end of B cell development. *Nat. Immunol.* 2:1103–1108. http://dx.doi.org/10.1038/ni1201-1103

Casellas, R., T.A. Shih, M. Kleinewietfeld, J. Rakonjac, D. Nemazee, K. Rajewsky, and M.C. Nussenzweig. 2001. Contribution of receptor editing to the antibody repertoire. *Science.* 291:1541–1544. http://dx.doi.org/10.1126/science.1056600

Casellas, R., Q. Zhang, N.Y. Zheng, M.D. Mathias, K. Smith, and P.C. Wilson. 2007. Igκ allelic inclusion is a consequence of receptor editing. *J. Exp. Med.* 204:153–160. http://dx.doi.org/10.1084/jem.20061918

Chan, O., and M.J. Shlomchik. 1998. A new role for B cells in systemic autoimmunity: B cells promote spontaneous T cell activation in MRL-lpr/lpr mice. *J. Immunol.* 160:51–59.

Chan, O.T., M.P. Madaio, and M.J. Shlomchik. 1999. B cells are required for lupus nephritis in the polygenic, Fas-intact MRL model of systemic autoimmunity. *J. Immunol.* 163:3592–3596.

Cohen, P.L., and R.A. Eisenberg. 1991. Lpr and gld: single gene models of systemic autoimmunity and lymphoproliferative disease. *Annu. Rev. Immunol.* 9:243–269. http://dx.doi.org/10.1146/annurev.iy.09.040191.001331

Dattamajumdar, A.K., D.P. Jacobson, L.E. Hood, and G.E. Osman. 1996. Rapid cloning of any rearranged mouse immunoglobulin variable genes. *Immunogenetics.* 43:141–151. http://dx.doi.org/10.1007/BF00176675

Fisher, C.L., R.A. Eisenberg, and P.L. Cohen. 1988. Quantitation and IgG subclass distribution of antichromatin autoantibodies in SLE mice. *Clin. Immunol. Immunopathol.* 46:205–213. http://dx.doi.org/10.1016/0090-1229(88)90183-3

Gerdes, T., and M. Wabl. 2004. Autoreactivity and allelic inclusion in a B cell nuclear transfer mouse. *Nat. Immunol.* 5:1282–1287. http://dx.doi.org/10.1038/ni1133

Giachino, C., E. Padovan, and A. Lanzavecchia. 1995. κ$^+$λ$^+$ dual receptor B cells are present in the human peripheral repertoire. *J. Exp. Med.* 181:1245–1250. http://dx.doi.org/10.1084/jem.181.3.1245

Goodnow, C.C., J. Sprent, B. Fazekas de St Groth, and C.G. Vinuesa. 2005. Cellular and genetic mechanisms of self tolerance and autoimmunity. *Nature.* 435:590–597. http://dx.doi.org/10.1038/nature03724

Grandien, A., R. Fucs, A. Nobrega, J. Andersson, and A. Coutinho. 1994. Negative selection of multireactive B cell clones in normal adult mice. *Eur. J. Immunol.* 24:1345–1352. http://dx.doi.org/10.1002/eji.1830240616

Halverson, R., R.M. Torres, and R. Pelanda. 2004. Receptor editing is the main mechanism of B cell tolerance toward membrane antigens. *Nat. Immunol.* 5:645–650. http://dx.doi.org/10.1038/ni1076

Harris, J.F., R.G. Hawley, T.S. Hawley, and G.C. Crawford-Sharpe. 1992. Increased frequency of both total and specific monoclonal antibody

producing hybridomas using a fusion partner that constitutively expresses recombinant IL-6. *J. Immunol. Methods*. 148:199–207. http://dx.doi.org/10.1016/0022-1759(92)90173-Q

Herlands, R.A., J. William, U. Hershberg, and M.J. Shlomchik. 2007. Anti-chromatin antibodies drive in vivo antigen-specific activation and somatic hypermutation of rheumatoid factor B cells at extrafollicular sites. *Eur. J. Immunol.* 37:3339–3351. http://dx.doi.org/10.1002/eji.200737752

Herlands, R.A., S.R. Christensen, R.A. Sweet, U. Hershberg, and M.J. Shlomchik. 2008. T cell-independent and toll-like receptor-dependent antigen-driven activation of autoreactive B cells. *Immunity*. 29:249–260. http://dx.doi.org/10.1016/j.immuni.2008.06.009

Hippen, K.L., B.R. Schram, L.E. Tze, K.A. Pape, M.K. Jenkins, and T.W. Behrens. 2005. In vivo assessment of the relative contributions of deletion, anergy, and editing to B cell self-tolerance. *J. Immunol.* 175:909–916.

Huang, H., J.F. Kearney, M.J. Grusby, C. Benoist, and D. Mathis. 2006. Induction of tolerance in arthritogenic B cells with receptors of differing affinity for self-antigen. *Proc. Natl. Acad. Sci. USA*. 103:3734–3739. http://dx.doi.org/10.1073/pnas.0600214103

Izui, S., V.E. Kelley, K. Masuda, H. Yoshida, J.B. Roths, and E.D. Murphy. 1984. Induction of various autoantibodies by mutant gene lpr in several strains of mice. *J. Immunol.* 133:227–233.

Kalinina, O., C.M. Doyle-Cooper, J. Miksanek, W. Meng, E.L. Prak, and M.G. Weigert. 2011. Alternative mechanisms of receptor editing in autoreactive B cells. *Proc. Natl. Acad. Sci. USA*. 108:7125–7130. http://dx.doi.org/10.1073/pnas.1019389108

Kamogawa, J., M. Terada, S. Mizuki, M. Nishihara, H. Yamamoto, S. Mori, Y. Abe, K. Morimoto, S. Nakatsuru, Y. Nakamura, and M. Nose. 2002. Arthritis in MRL/lpr mice is under the control of multiple gene loci with an allelic combination derived from the original inbred strains. *Arthritis Rheum*. 46:1067–1074. http://dx.doi.org/10.1002/art.10193

Kenny, J.J., L.J. Rezanka, A. Lustig, R.T. Fischer, J. Yoder, S. Marshall, and D.L. Longo. 2000. Autoreactive B cells escape clonal deletion by expressing multiple antigen receptors. *J. Immunol.* 164:4111–4119.

Lam, K.P., R. Kühn, and K. Rajewsky. 1997. In vivo ablation of surface immunoglobulin on mature B cells by inducible gene targeting results in rapid cell death. *Cell*. 90:1073–1083. http://dx.doi.org/10.1016/S0092-8674(00)80373-6

Lamoureux, J.L., L.C. Watson, M. Cherrier, P. Skog, D. Nemazee, and A.J. Feeney. 2007. Reduced receptor editing in lupus-prone MRL/lpr mice. *J. Exp. Med.* 204:2853–2864. http://dx.doi.org/10.1084/jem.20071268

Langman, R., and M. Cohn. 2002. Haplotype exclusion: the solution to a problem in natural selection. *Semin. Immunol.* 14:153–162, discussion :229–247. http://dx.doi.org/10.1016/S1044-5323(02)00039-8

Li, H., Y. Jiang, E.L. Prak, M. Radic, and M. Weigert. 2001. Editors and editing of anti-DNA receptors. *Immunity*. 15:947–957. http://dx.doi.org/10.1016/S1074-7613(01)00251-5

Li, Y., H. Li, D. Ni, and M. Weigert. 2002a. Anti-DNA B cells in MRL/lpr mice show altered differentiation and editing pattern. *J. Exp. Med.* 196:1543–1552. http://dx.doi.org/10.1084/jem.20021560

Li, Y., H. Li, and M. Weigert. 2002b. Autoreactive B cells in the marginal zone that express dual receptors. *J. Exp. Med.* 195:181–188. http://dx.doi.org/10.1084/jem.20011453

Li, Y., F. Chen, M. Putt, Y.K. Koo, M. Madaio, J.C. Cambier, P.L. Cohen, and R.A. Eisenberg. 2008. B cell depletion with anti-CD79 mAbs ameliorates autoimmune disease in MRL/lpr mice. *J. Immunol.* 181:2961–2972.

Liang, Z., S. Chang, M.S. Youn, and C. Mohan. 2009. Molecular hallmarks of anti-chromatin antibodies associated with the lupus susceptibility locus, Sle1. *Mol. Immunol.* 46:2671–2681. http://dx.doi.org/10.1016/j.molimm.2008.12.034

Liu, S., M.G. Velez, J. Humann, S. Rowland, F.J. Conrad, R. Halverson, R.M. Torres, and R. Pelanda. 2005. Receptor editing can lead to allelic inclusion and development of B cells that retain antibodies reacting with high avidity autoantigens. *J. Immunol.* 175:5067–5076.

Mandik-Nayak, L., S.J. Seo, C. Sokol, K.M. Potts, A. Bui, and J. Erikson. 1999. MRL-lpr/lpr mice exhibit a defect in maintaining developmental arrest and follicular exclusion of anti–double-stranded DNA B cells. *J. Exp. Med.* 189:1799–1814. http://dx.doi.org/10.1084/jem.189.11.1799

Merrell, K.T., R.J. Benschop, S.B. Gauld, K. Aviszus, D. Decote-Ricardo, L.J. Wysocki, and J.C. Cambier. 2006. Identification of anergic B cells within a wild-type repertoire. *Immunity*. 25:953–962. http://dx.doi.org/10.1016/j.immuni.2006.10.017

Nemazee, D. 2006. Receptor editing in lymphocyte development and central tolerance. *Nat. Rev. Immunol.* 6:728–740. http://dx.doi.org/10.1038/nri1939

Nose, M., M. Nishimura, M.R. Ito, J. Toh, T. Shibata, and T. Sugisaki. 1996. Arteritis in a novel congenic strain of mice derived from MRL/Lpr lupus mice: genetic dissociation from glomerulonephritis and limited autoantibody production. *Am. J. Pathol.* 149:1763–1769.

Nossal, G.J., and O. Makela. 1962. Kinetic studies on the incidence of cells appearing to form two antibodies. *J. Immunol.* 88:604–612.

Odegard, J.M., B.R. Marks, L.D. DiPlacido, A.C. Poholek, D.H. Kono, C. Dong, R.A. Flavell, and J. Craft. 2008. ICOS-dependent extrafollicular helper T cells elicit IgG production via IL-21 in systemic autoimmunity. *J. Exp. Med.* 205:2873–2886. http://dx.doi.org/10.1084/jem.20080840

Oracki, S.A., J.A. Walker, M.L. Hibbs, L.M. Corcoran, and D.M. Tarlinton. 2010. Plasma cell development and survival. *Immunol. Rev.* 237:140–159. http://dx.doi.org/10.1111/j.1600-065X.2010.00940.x

Orlandi, R., D.H. Güssow, P.T. Jones, and G. Winter. 1989. Cloning immunoglobulin variable domains for expression by the polymerase chain reaction. *Proc. Natl. Acad. Sci. USA*. 86:3833–3837. http://dx.doi.org/10.1073/pnas.86.10.3833

Ozato, K., N. Mayer, and D.H. Sachs. 1980. Hybridoma cell lines secreting monoclonal antibodies to mouse H-2 and Ia antigens. *J. Immunol.* 124:533–540.

Panigrahi, A.K., N.G. Goodman, R.A. Eisenberg, M.R. Rickels, A. Naji, and E.T. Luning Prak. 2008. RS rearrangement frequency as a marker of receptor editing in lupus and type 1 diabetes. *J. Exp. Med.* 205:2985–2994. http://dx.doi.org/10.1084/jem.20082053

Pauza, M.E., J.A. Rehmann, and T.W. LeBien. 1993. Unusual patterns of immunoglobulin gene rearrangement and expression during human B cell ontogeny: human B cells can simultaneously express cell surface κ and λ light chains. *J. Exp. Med.* 178:139–149. http://dx.doi.org/10.1084/jem.178.1.139

Pelanda, R., and R.M. Torres. 2006. Receptor editing for better or for worse. *Curr. Opin. Immunol.* 18:184–190. http://dx.doi.org/10.1016/j.coi.2006.01.005

Pelanda, R., and R. Torres. 2012. Central B-cell tolerance: where selection begins. *Cold Spring Harb. Perspect. Biol.* 4:a007146. http://dx.doi.org/10.1101/cshperspect.a007146

Peterson, L.K., D. Wells, L. Shaw, M.G. Velez, R. Harbeck, and L.L. Dragone. 2009. Novel method for quantitative ANA measurement using near-infrared imaging. *J. Immunol. Methods*. 349:1–8. http://dx.doi.org/10.1016/j.jim.2009.08.010

Rankin, A.L., H. Guay, D. Herber, S.A. Bertino, T.A. Duzanski, Y. Carrier, S. Keegan, M. Senices, N. Stedman, M. Ryan, et al. 2012. IL-21 receptor is required for the systemic accumulation of activated B and T lymphocytes in MRL/MpJ-Fas(lpr/lpr)/J mice. *J. Immunol.* 188:1656–1667. http://dx.doi.org/10.4049/jimmunol.1003871

Ratkay, L.G., B. Tait, J. Tonzetich, and J.D. Waterfield. 1994. Lpr and MRL background gene involvement in the control of adjuvant enhanced arthritis in MRL-lpr mice. *J. Autoimmun.* 7:561–573. http://dx.doi.org/10.1006/jaut.1994.1041

Reth, M., G.J. Hämmerling, and K. Rajewsky. 1978. Analysis of the repertoire of anti-NP antibodies in C57BL/6 mice by cell fusion. I. Characterization of antibody families in the primary and hyperimmune response. *Eur. J. Immunol.* 8:393–400. http://dx.doi.org/10.1002/eji.1830080605

Rezanka, L.J., J.J. Kenny, and D.L. Longo. 2005. Dual isotype expressing B cells [kappa(+)/lambda(+)] arise during the ontogeny of B cells in the bone marrow of normal nontransgenic mice. *Cell. Immunol.* 238:38–48. http://dx.doi.org/10.1016/j.cellimm.2005.12.004

Roark, J.H., C.L. Kuntz, K.A. Nguyen, A.J. Caton, and J. Erikson. 1995a. Breakdown of B cell tolerance in a mouse model of systemic lupus erythematosus. *J. Exp. Med.* 181:1157–1167. http://dx.doi.org/10.1084/jem.181.3.1157

Roark, J.H., C.L. Kuntz, K.A. Nguyen, L. Mandik, M. Cattermole, and J. Erikson. 1995b. B cell selection and allelic exclusion of an anti-DNA Ig transgene in MRL-lpr/lpr mice. *J. Immunol.* 154:4444–4455.

Rordorf-Adam, C., D. Serban, A. Pataki, and M. Grüninger. 1985. Serum amyloid P component and autoimmune parameters in the assessment of arthritis activity in MRL/lpr/lpr mice. *Clin. Exp. Immunol.* 61: 509–516.

Rowland, S.L., C.L. DePersis, R.M. Torres, and R. Pelanda. 2010a. Ras activation of Erk restores impaired tonic BCR signaling and rescues immature B cell differentiation. *J. Exp. Med.* 207:607–621. http://dx.doi.org/10.1084/jem.20091673

Rowland, S.L., K.F. Leahy, R. Halverson, R.M. Torres, and R. Pelanda. 2010b. BAFF receptor signaling aids the differentiation of immature B cells into transitional B cells following tonic BCR signaling. *J. Immunol.* 185:4570–4581. http://dx.doi.org/10.4049/jimmunol.1001708

Rubtsov, A.V., K. Rubtsova, A. Fischer, R.T. Meehan, J.Z. Gillis, J.W. Kappler, and P. Marrack. 2011. Toll-like receptor 7 (TLR7)-driven accumulation of a novel CD11c^{+} B-cell population is important for the development of autoimmunity. *Blood.* 118:1305–1315. http://dx.doi.org/10.1182/blood-2011-01-331462

Samuels, J., Y.S. Ng, C. Coupillaud, D. Paget, and E. Meffre. 2005. Impaired early B cell tolerance in patients with rheumatoid arthritis. *J. Exp. Med.* 201:1659–1667. http://dx.doi.org/10.1084/jem.20042321

Schlissel, M.S. 2003. Regulating antigen-receptor gene assembly. *Nat. Rev. Immunol.* 3:890–899. http://dx.doi.org/10.1038/nri1225

Shlomchik, M.J. 2008. Sites and stages of autoreactive B cell activation and regulation. *Immunity.* 28:18–28. http://dx.doi.org/10.1016/j.immuni.2007.12.004

Theofilopoulos, A.N., and F.J. Dixon. 1985. Murine models of systemic lupus erythematosus. *Adv. Immunol.* 37:269–390. http://dx.doi.org/10.1016/S0065-2776(08)60342-9

Velez, M.G., M. Kane, S. Liu, S.B. Gauld, J.C. Cambier, R.M. Torres, and R. Pelanda. 2007. Ig allotypic inclusion does not prevent B cell development or response. *J. Immunol.* 179:1049–1057.

Vettermann, C., and M.S. Schlissel. 2010. Allelic exclusion of immunoglobulin genes: models and mechanisms. *Immunol. Rev.* 237:22–42. http://dx.doi.org/10.1111/j.1600-065X.2010.00935.x

Wang, H., and M.J. Shlomchik. 1998. Maternal Ig mediates neonatal tolerance in rheumatoid factor transgenic mice but tolerance breaks down in adult mice. *J. Immunol.* 160:2263–2271.

Wardemann, H., S. Yurasov, A. Schaefer, J.W. Young, E. Meffre, and M.C. Nussenzweig. 2003. Predominant autoantibody production by early human B cell precursors. *Science.* 301:1374–1377. http://dx.doi.org/10.1126/science.1086907

Warren, R.W., S.A. Caster, J.B. Roths, E.D. Murphy, and D.S. Pisetsky. 1984. The influence of the lpr gene on B cell activation: differential antibody expression in lpr congenic mouse strains. *Clin. Immunol. Immunopathol.* 31:65–77. http://dx.doi.org/10.1016/0090-1229(84)90190-9

Watanabe-Fukunaga, R., C.I. Brannan, N.G. Copeland, N.A. Jenkins, and S. Nagata. 1992. Lymphoproliferation disorder in mice explained by defects in Fas antigen that mediates apoptosis. *Nature.* 356:314–317. http://dx.doi.org/10.1038/356314a0

Wen, L., J. Brill-Dashoff, S.A. Shinton, M. Asano, R.R. Hardy, and K. Hayakawa. 2005. Evidence of marginal-zone B cell-positive selection in spleen. *Immunity.* 23:297–308. http://dx.doi.org/10.1016/j.immuni.2005.08.007

William, J., C. Euler, and M.J. Shlomchik. 2005. Short-lived plasmablasts dominate the early spontaneous rheumatoid factor response: differentiation pathways, hypermutating cell types, and affinity maturation outside the germinal center. *J. Immunol.* 174:6879–6887.

Yurasov, S., H. Wardemann, J. Hammersen, M. Tsuiji, E. Meffre, V. Pascual, and M.C. Nussenzweig. 2005. Defective B cell tolerance checkpoints in systemic lupus erythematosus. *J. Exp. Med.* 201:703–711. http://dx.doi.org/10.1084/jem.20042251

Yurasov, S., T. Tiller, M. Tsuiji, K. Velinzon, V. Pascual, H. Wardemann, and M.C. Nussenzweig. 2006. Persistent expression of autoantibodies in SLE patients in remission. *J. Exp. Med.* 203:2255–2261. http://dx.doi.org/10.1084/jem.20061446